environmental microbiology

Environmental Microbiology (2022) **24**(1), 370–389 doi:10.1111/1462-2920.15852

Sulfidic acetate mineralization at 45°C by an aquifer microbial community: key players and effects of heat changes on activity and community structure

Mohammad S. Bin Hudari, Carsten Vogt* and Hans H. Richnow

Department of Isotope Biogeochemistry, Helmholtz Centre for Environmental Research – UFZ, Leipzig, Germany.

Summary

High-Temperature Aquifer Thermal Energy Storage (HT-ATES) is a sustainable approach for integrating thermal energy from various sources into complex energy systems. Temperatures ≥45°C, which are relevant in impact zones of HT-ATES systems, may dramatically influence the structure and activities of indigenous aquifer microbial communities. Here, we characterized an acetate-mineralizing, sulfate-reducing microbial community derived from an aquifer and adapted to 45°C. Acetate mineralization was strongly inhibited at temperatures ≤25°C and 60°C. Prolonged incubation at 12°C and 25°C resulted in acetate mineralization recovery after 40–80 days whereas acetate was not mineralized at 60°C within 100 days. Cultures pre-grown at 45°C and inhibited for 28 days by incubation at 12°C, 25°C, or 60°C recovered quickly after changing the temperature back to 45°C. Phylotypes affiliated to the order *Spirochaetales* and to endospore-forming sulfate reducers of the order *Clostridiales* were highly abundant in microcosms being active at 45°C highlighting their key role. In summary, prolonged incubation at 45°C resulted in active microbial communities mainly consisting of organisms adapted to temperatures between the typical temperature range of mesophiles and thermophiles and being resilient to temporary heat changes.

Introduction

A considerable part of fossil fuels is globally consumed for heating and cooling purposes (Elsland *et al*., 2017; Heatroadmapeurope, 2019). Aquifer Thermal Energy Storage (ATES) promises a more sustainable supply of thermal energy by storing and extracting heat in the subsurface. In addition to storing thermal energy from heat-generating industries such as incineration plants, ATES can operate in seasonal mode, by storing excess thermal energy in aquifers during the summer, which can then be used during the cooler months. More than 90% of ATES in operation worldwide are located in Europe (Fleuchaus *et al*., 2018). A majority of the ATES in operation are Low-Temperature (LT-ATES) installations, which function under an upper limit temperature threshold (e.g. 25°C). However, by operation of High-Temperature ATES (HT-ATES) systems with storage temperatures >40°C, an integration of (non-)renewable heat sources into complex energy systems is possible (Fleuchaus *et al*., 2020). Some of the limitations that contribute to the lower adoption of HT-ATES largely stem from long-term operational costs, uncertainty on their environmental impact, and regulation issues (Fleuchaus *et al*., 2018; Fleuchaus *et al*., 2020).

ATES is especially attractive for urban or industrial areas due to its high energy production and consumption. Aquifers in those sites are often contaminated by organic pollutants (National Research Council, 2000), and combining remediation techniques with ATES is an attractive approach. As groundwater temperatures within the ATES core zone and vicinity are affected, this will influence a contaminant's physicochemical characteristics and its attenuation potential. Petroleum hydrocarbons constitute the most common contaminants introduced into the subsurface through leakage or improper disposal (Rooney-Varga *et al*., 1999; Da Silva and Alvarez, 2004; Vogt *et al*., 2007). Both biotic and abiotic attenuation of contaminants can occur, but the latter contribution tends to be limited in aquifers, where oxygen is rapidly depleted (USEPA, 1999; Meckenstock *et al*., 2015). During syntrophic hydrocarbon degradation, acetate is a commonly occurring intermediate in the several pathways reported (Jones *et al*., 2008; Gieg *et al*., 2010; Fuchs, 2011; Lueders, 2017). In the presence of terminal electron acceptors, acetate can serve both as carbon source

Received 9 August, 2021; revised 9 November, 2021; accepted 12 November, 2021. *For correspondence. E-mail carsten.vogt@ufz.de; Tel. +49 341 235 1357; Fax: +49 341 235 450822.

and electron donor becoming mineralized to carbon dioxide (Wu *et al*., 1997; Ho *et al*., 2002; Heuer *et al*., 2010; Head *et al*., 2014). Due to the availability of sulfate in various ecosystems, dissimilatory sulfate reduction is among the most commonly described metabolism under anoxic conditions (National Research Council, 2000; Miao *et al*., 2012).

In an ecosystem comprising a plethora of microorganisms, microbial processes are not as straightforward as correlating biotransformation with the Arrhenius equation (Garcia *et al*., 2018). The growth temperature, which is an intrinsic characteristic of each species, is defined by the maxima, minima and optima, which connect microbial growth to temperature (Dettmer, 2002). Maximal growth rates can be achieved around the optimal temperature, whereas at higher temperatures rates rapidly decrease and cease under sub-optimal conditions (Mohr and Krawiec, 1980; Huang *et al*., 2011). For instance, this can be observed with the different microbial growth ranges in psychrophiles (0–20°C), mesophiles (8–48°C), thermophiles (40–70°C) and hyperthermophiles (65–90°C) (Madigan *et al*., 2017). Heterogeneity and localized niches can also affect attenuation processes (Tian *et al*., 2017; Garcia *et al*., 2018; Pannekens *et al*., 2019). The effects of temperature are thus multi-faceted, since temperature does not just affect physicochemical characteristics of the contaminants (Koproch *et al*., 2019), but it can also affect the microbial community and the biotransformation processes (Dettmer, 2002; Higashioka *et al*., 2011). Temperature fluctuations arising from injection and extraction of water into aquifers could largely influence the general activity of the microbial community as well the ability to mineralize distinct contaminants (Hossain *et al*., 2017).

In a previous study (Bin Hudari *et al*., 2020), using a hydrocarbon-degrading microbial community spiked with uniformly ^{13}C-labelled acetate under sulfate reducing condition, acetate mineralization was observed at 12°C, 25°C and 38°C, whereas acetate was not mineralized at 60°C and 80°C, while only one of three replicates incubated at 45°C mineralized acetate with concomitant sulfide production. In that study, 45°C was selected, because it lies in the overlap of mesophilic-thermophilic growth boundary (Madigan *et al*., 2017), which could potentially harbor a niche group of heat-tolerant microorganisms. In an HT-ATES system, 45°C can be found either in the core zone or in the outer impact zone (Sanner *et al*., 2005; Lerm *et al*., 2013; Kallesøe and Vangkilde-Pedersen, 2019). This could also influence the surrounding zone which is in close proximity to the core by indirectly enhancing bioremediation activity (Todorov *et al*., 2020). If bioremediation activity can be sustained at this temperature (45°C), this would be an extra advantage in addition to allowing a greater thermal energy capacity with the implementation of HT-ATES. While there have been studies to assess the likely impacts of temperature in ATES (Jesußek *et al*., 2012; Jesußek *et al*., 2013; Ni *et al*., 2015) as well as in other applications (Deeb and Alvarez-Cohen, 1999; Friis *et al*., 2007a,b,c; Yadav *et al*., 2012; Zeman *et al*., 2014), studies on the effects of periodic heat storage subject to different temperature exposure on biotransformation are limited. Therefore, our microcosm-based study aims to explore the effects of periodic heat exchange on acetate mineralization, sulfide production, their rates and microbial community composition. Starting with an inoculum comprising an aquifer microbial community enriched at 45°C, microcosms were subjected to different treatment regimes within three scenarios: (i) 'control' at 45°C, (ii) 'adaptation' from 45°C to 12°C, 25°C, or 60°C and incubated for up to 133 days and (iii) 'heat exchange' scenario where microcosms were temporarily exposed to 12°C, 25°C, 38°C, or 60°C for a 28-day period before switching again to 45°C.

Results

Activities at 45°C and after subsequent permanent temperature shifts to 12°C, 25°C or 60°C

These experiments were done to determine general activity parameter at 45°C, to characterize the activities of the 45°C-adapted community at lower and higher temperatures ($\Delta T \geq 15$°C) and to determine the resilience of the community to mineralize acetate at lower and higher temperatures after prolonged incubation. In microcosms incubated continuously at 45°C (treatment 1), acetate was mineralized in all three replicates with concomitant sulfide production and no apparent lag phase (Fig. 1A and B). Within the first 6.25 days, acetate was mineralized at an average rate of 52.9 $\pm$ 8.5 μM d^{-1} while sulfide was produced at an average rate of 51.8 $\pm$ 3.8 μM d^{-1}. Subsequently, both rates increased to 85.4 $\pm$ 17.3 (mineralization) and 65.7 $\pm$ 2.9 μM d^{-1} (sulfide production), indicating increasing cell numbers by growth. After 10 days of incubation, 87.5 $\pm$ 17.7% (875.4 $\pm$ 177 μM) of the added acetate was mineralized accompanied by production of 657.4 $\pm$ 29 μM sulfide (Tables 1 and S3).

In treatments 2–4 of the 'adaptation scenario', average acetate mineralization and sulfide production rates during the 'Pre' stage at 45°C were comparable to treatment 1 values (Table 1). Transferring the communities to either 12°C, 25°C or 60°C resulted in significantly changing mineralization and sulfide production rates; generally, the selected temperatures caused an immediate inhibition of activity. A temperature of 12°C (treatment 2, 45 → 12°C) completely inhibited acetate mineralization for around 63 days; thereafter, only two of three replicates mineralized acetate at a rate of 13.9 $\pm$ 1.4 μM d^{-1} and produced sulfide at 11.6 $\pm$ 1.7 μM d^{-1} (Table 1, Fig. 1C and D, Table S3).

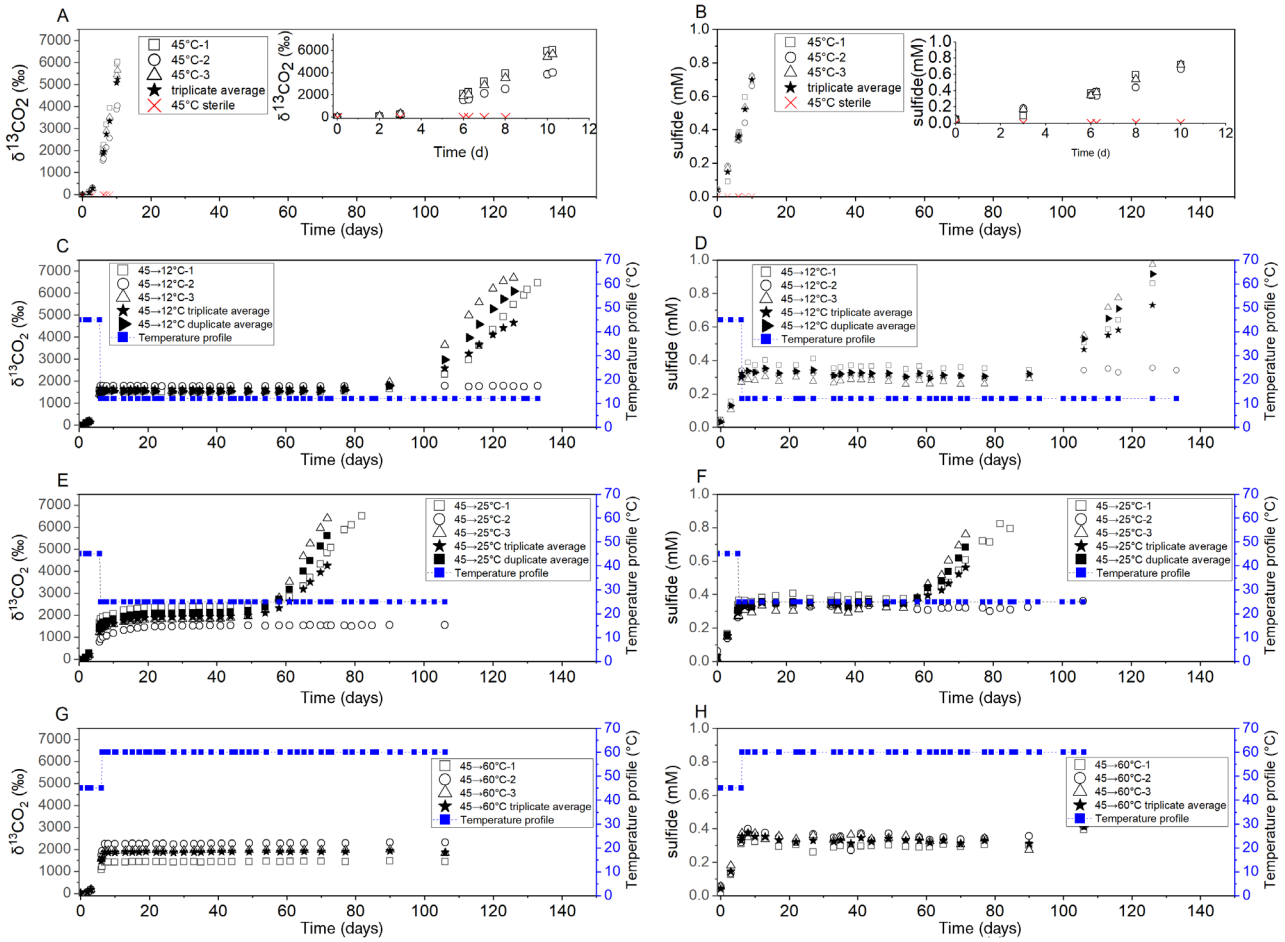

Fig. 1. Time courses development of ^{13}C-labelled CO_2 and sulfide for treatments 1 (45°C) (A, B), 2 (45 → 12°C) (C, D), 3 (45 → 25°C) (E, F) and 4 (45 → 60°C) (G, H) respectively. Additional insert in diagrams in A and B represent the data for the first twelve days of incubation at higher resolution. Data are presented for each respective replicate and the corresponding average of these replicates.

Shifting the temperature to 25°C (treatment 3, 45 → 25°C) did not completely inhibit acetate mineralization as observed for 12°C, but rates were tremendously decreased (Table 1, Fig. 1E and F). After more than 50 days incubation at 25°C ('End' stage), acetate mineralization and sulfide production started to increase again in two of three replicates at rates of 11.3 ± 1.7 and 6.7 ± 0.9 μM d^{-1} respectively (Table 1, Fig. 1E and F). The third replicate was excluded as mineralization ceased after a few days at 25°C (Fig. 1E, Table S3). Transferring the communities to a temperature of 60°C (treatment 4, 45 → 60°C) completely inhibited mineralization and sulfide production after some residual activity within the immediate 0.75 days after shifting to 60°C (Table 1, Fig. 1G and H; Table S3).

Activities at 45°C after temporary temperature shifts to 12°C, 25°C, 38°C or 60°C

These experiments were done to determine the resilience of the 45°C-adapted community to temporary lower or higher temperatures ($\Delta T \geq 7$°C). In the heat exchange setups (treatments 5–8), communities were first incubated at 45°C for 6 days ('Pre' stage), and then transferred to 12°C (treatment 5), 25°C (treatment 6), 38°C (treatment 7) or 60°C (treatment 8) for up to 28 days. On day 35, they were returned to 45°C ('Post' stage). In the 'Pre' stage, all replicates mineralized acetate and produced sulfide without lag-phase in similar rates as described for the permanent temperature shift experiments (Tables 1 and 2; Figs 1A and B, 2A–D, and 3A–D).

When replicates were transferred to the respective incubation temperature after 6 days ('Post' stage), acetate mineralization and sulfide production rates varied depending on the selected new temperature; in general, cultures behaved similarly to those observed for treatments 2–4. During the 29-day incubation at 12°C, acetate mineralization was not observed (treatment 5, Fig. 2A) while some residual activity was observed at 60°C, shortly after temperature change (5.0 ± 0.2 μM,

Table 1. Overview on results of triplicates averages of acetate mineralization, sulfide production and rates for treatments 1–4.

Objective	Control		Adaptation			
Treatment	1		Treatment	2	3	4
Batch	45°C	Stage	Batch	45 → 12°C	45 → 25°C	45 → 60°C
Duration(d)	6.25	Pre	Duration (d)	6.25	6.25	6.25
Acetate mineralized (%)	33.1 ± 5.3		Acetate mineralized (%)	27.4 ± 2.2	23.0 ± 7.6	27.1 ± 6.0
Acetate mineralized (μM)	330.9 ± 53.4		Acetate mineralized (μM)	274.2 ± 22.2	230.3 ± 76.0	270.8 ± 59.8
Rate at $t = 6.25$ (μM acetate d^{-1})	52.9 ± 8.5		Rate at $t = 6.25$ (μM acetate d^{-1})	43.8 ± 3.5	36.8 ± 12.2	43.3 ± 9.6
Duration (d)	6.25		Duration (d)	6.25	6.25	6.25
Sulfide produced (μM)	323.9 ± 23.6		Sulfide produced (μM)	292.3 ± 2.4	279.0 ± 56.0	313.1 ± 7.4 ($n = 3$)
Rate at $t = 6.25$ (μM sulfide d^{-1})	51.8 ± 3.8		Rate (μM d^{-1})	47.4 ± 1.0	44.6 ± 9.0	50.1 ± 1.2 ($n = 3$)
Duration (d)	10.25	Post	Duration (d)	56–63	31.75–75.75	75.75[a.]
Acetate mineralized (%)	87.5 ± 17.7		Acetate mineralized (%)	82.3 ± 1.6 ($n = 2$)	56.4 ± 40.1 ($n = 3$)	4.3 ± 1.0[a., c.]
Acetate mineralized (μM)	875.4 ± 176.9				79.5 ± 4.3 ($n = 2$)	
Rate (μM acetate d^{-1})	85.4 ± 17.3		Lag phase for acetate mineralization after temperature shift based on $\delta^{13}CO_2$ (d)	63.75	Not observed[b.]	-
Duration (d)	10		Acetate mineralized (μM)	822.7 ± 16.1 ($n = 2$)	564.5 ± 401.0 ($n = 3$)	42.8 ± 10.4
Sulfide produced (μM)	657.4 ± 29.0				795.4 ± 43.2 ($n = 2$)	
Rate (μM sulfide d^{-1})	65.7 ± 2.9		Rate (μM acetate d^{-1})	13.9 ± 1.45 ($n = 2$)	8.6 ± 4.8 ($n = 3$)	-[a.]
					11.3 ± 1.7 ($n = 2$)	
Sulfide produced/acetate mineralized (end of incubation)	0.77 ± 0.1		Duration (d)	56 & 63 ($n = 2$)	65.75 & 75.75 ($n = 2$)[d.]	-
			Sulfide produced (μM)	685.5 ± 41.2 ($n = 2$)	471.4 ± 19.3 ($n = 2$)[d.]	-
			Rate (μM d^{-1})	11.6 ± 1.7 ($n = 2$)	6.7 ± 0.9 ($n = 2$)[d.]	-[a.]

[a.]Acetate mineralization or sulfide production ceased, therefore corresponding rates were not calculated.
[b.]Mineralization was continuous but proceeded at low rate initially when transferred to 25°C, rates increased after longer incubation at 25°C (see Fig. 1E).
[c.]Acetate mineralization or sulfide production due to residual activity after shifting to 60°C.
[d.]Third replicate not considered, information in Table S3.

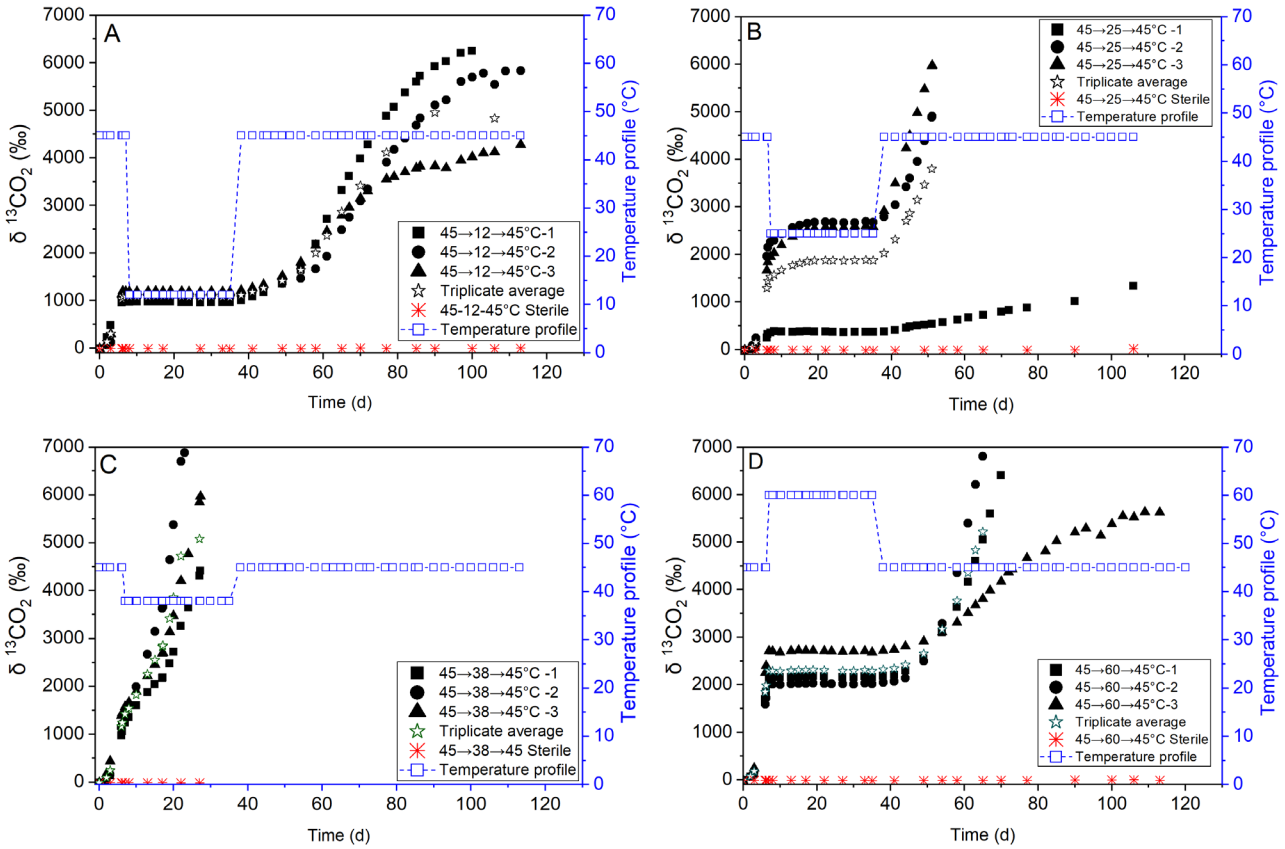

Fig. 2. Time courses of the development of ^{13}C-labelled CO_2 production from microcosms in treatments 5 (45° → 12 → 45°C) (A), 6 (45 → 25 → 45°C) (B), 7 (45 → 38°C) (C) and 8 (45 → 60 → 45°C) (D). In treatment 7, the experiment was completed during incubation at 38°C and was not returned to 45°C.

treatment 8, Fig. 2A). Sulfide production was not observed at both temperatures (Fig. 3A and D; Table S3). At 25°C (treatment 6), acetate mineralization phased out after 14 days and was afterward absent, with only 9.6 ± 8.3 μM ($n = 3$) acetate mineralized and similar small amounts of sulfide produced (Figs 2B and 3B, Table S3). In contrast, during incubation at 38°C (treatment 7), mineralization continued with no lag phase and was completed 16–21 days after shifting to the new temperature, and hence was not returned to 45°C (Fig. 2C, Table 2). Acetate was mineralized (742.4 ± 189.3 μM) at a rate of 39.1 ± 15 μM d^{-1}, while an average of 449 ± 80.2 μM sulfide was produced at 22.4 ± 5.5 μM d^{-1} (Table 2). Both rates were lower with respect to the control which was continuously incubated at 45°C (treatment 1, Table 1). Acetate mineralization rates were initially slightly lower as observed for 45°C when the replicates were placed at 38°C; however, the rates increased again with prolonged incubation at 38°C (Fig. 2C), where rates during incubation at 38°C were comparable to rates before temperature change at 45°C (Table 2), indicating growth of the acetate-mineralizing community.

At $t = 35$ days, treatments 5 (12°C), 6 (25°C) and 8 (60°C) were returned to 45°C. Acetate mineralization resumed in all three treatments, albeit at different rates (Fig. 2A, B, and D), alongside sulfide production (Fig. 3A, B, and D). Based on $\delta^{13}CO_2$ values, lag phases were not evident in all three treatments (Table S3). In treatment 5 (12°C), triplicate communities mineralized 722.8 ± 189 μM acetate at 10 ± 3.4 μM d^{-1} when returned to 45°C, while 591.2 ± 127.3 μM of sulfide was produced at a rate of 8.2 ± 1.6 μM d^{-1} (Table 2); these rates are about three to four times lower when compared to rates before temperature change at $t = 6.25$ d, indicating a negative effect of 12°C on the 45°C-adapted community. For treatment 6 (45 → 25 → 45°C), on average, 332.4 ± 168 μM of acetate was mineralized at 17.9 ± 14.4 μM d^{-1} ($n = 3$) with no lag phase after microcosms were returned to 45°C. One replicate recovered very slowly, with only 2.2 μM d^{-1} acetate mineralized and 1.7 μM sulfide d^{-1} produced in 71 days. These rates were around ten times lower when compared to the other two replicates (Table S3). The average acetate mineralization and sulfide production rates at 45°C after the temporary incubation at 25°C were about two times lower

Table 2. Overview on results of triplicates averages of acetate mineralization, sulfide production and rates for treatments 5–8.

Objective		Heat exchange			
	Treatment	5	6	7	8
Stage	Batch	45 → 12 → 45°C	45 → 25 → 45°C	45 → 38°C[a.]	45 → 60 → 45°C
Pre	Duration (d)	6.25	6.25	6.25	6.25
	Acetate mineralized (%)	18.4 ± 1.8	24.2 ± 16.3 ($n = 3$) 33.4 ± 3.17 ($n = 2$)	20.9 ± 3.13	33.3 ± 6.02
	Acetate mineralized (μM)	183.6 ± 18.7	241.7 ± 163.2 ($n = 3$) 334.7 ± 37.1 ($n = 2$)	208.9 ± 31.4	333.4 ± 60.2
	Rate (μM d^{-1})	29.4 ± 3.0	38.7 ± 26.1[b.]	33.4 ± 5.0	53.3 ± 9.6
	Duration (d)	6.25	6.25	6.25	6.25
	Sulfide produced (μM)	230.7 ± 49.0	288.4 ± 78.1	245.9 ± 16.6	336.4 ± 48.5
	Rate (μM d^{-1})	36.9 ± 7.8	46.1 ± 12.5	39.3 ± 2.6	53.8 ± 7.8
Post	Duration (d)	28.75	28.75	16.75–21	28.75
	Acetate mineralized (%) cc	Not observed	9.6 ± 8.3 ($n = 3$) 13.9 ± 5.1 ($n = 2$)	74.2 ± 18.9	5.0 ± 0.2
	Acetate mineralized (μM)	Not observed	95.9 ± 83.0 ($n = 3$) 139.2 ± 20.6 ($n = 2$)	742.4 ± 189.3	50.4 ± 1.8[c.]
	Rate (μM acetate d^{-1})	Not observed	3.3 ± 2.9[b.]	39.1 ± 15.0	n/c
	Duration (d)	28.75	28.75	18.75–21	28.75
	Sulfide produced (μM)	Not observed	12.3 ± 3.7 ($n = 2$)	449.0 ± 80.2	Not observed
	Rate (μMsulfide d^{-1})	Not observed	0.4 ± 0.1 ($n = 2$)[e.]	22.4 ± 5.5	n/c
End	Duration (d)	65–78	16.25–71	-	30–74
	Lag phase of acetate mineralization after temperature shift based on $\delta^{13}CO_2$ values (d)	Not observed	Not observed	-	Not observed
	Acetate mineralized (%)	72.3 ± 18.9	33.2 ± 16.8	Completed prior	65.0 ± 15.6
	Acetate mineralized (μM)	722.8 ± 189.8	332.4 ± 168.5	-	649.2 ± 156.0
	Rate (μM acetate d^{-1})	10.0 ± 3.4	17.9 ± 14.4	Completed prior	17.4 ± 13.1[b.]
	Duration (d)	71–74	16.25 ($n = 2$)[e.]	Completed prior	30–71
	Sulfide produced (μM)	591.2 ± 127.3	282.6 ± 76.9 ($n = 2$)	-	453.9 ± 34.2
	Rate (μM sulfide d^{-1})	8.2 ± 1.6	17.4 ± 4.7 ($n = 2$)	Completed prior	11.7 ± 5.3

[a.]Acetate mineralization was completed during incubation at 38°C, no return to 45°C.
[b.]Only averaged rate of triplicates shown.
[c.]Acetate mineralization due to residual activity after shifting to 60°C.
[d.]Rate based on acetate mineralization duration.
[e.]Third replicate not considered, information in Table S3.
n/c, not considered.

when compared to the initial average rate before the temperature change at $t = 6.25$ d.

In treatment 8 (45 → 60 → 45°C), while no mineralization was observed during 60°C incubation, mineralization and sulfide production resumed with no apparent lag phase when returned to 45°C on day 35 (Figs 2D and 3D). Acetate was mineralized and sulfide produced after return to 45°C in rates of 17.4 ± 13.1 ($n = 3$) and 11.7 ± 5.3 μM d^{-1} ($n = 3$) respectively (Table 2). These rates were about three to four times lower compared to rates before temperature change (Table 2).

Microbial community composition

The Miseq sequencing data of the 18 samples produced 1 270 196 16S rRNA gene sequence reads with average reads of 70 556 ± 16 103 per sample, with minimum and maximum sequence reads of 46 807 and 109 242 respectively. The amplicon sequence variants (ASVs) varied between 38 and 135 shown by the rarefaction curve of the unrarefied samples (Fig. S2). The total sequences per sample were considered in the microbial community composition, however, for diversity analyses, sequences were first rarefied to the minimum sequencing depth of 46 807 without significant loss to ASVs.

Community compositions at different temperature regimes

Four microcosms were sacrificed at the end of the treatment to investigate the community composition of replicates from treatments 1 (45°C), 2 (45 → 12°C), and 3 (45 → 25°C) at time points $t = 10$ d, 126 d and 82 d respectively (Fig. 1, Table S2), represented at the order

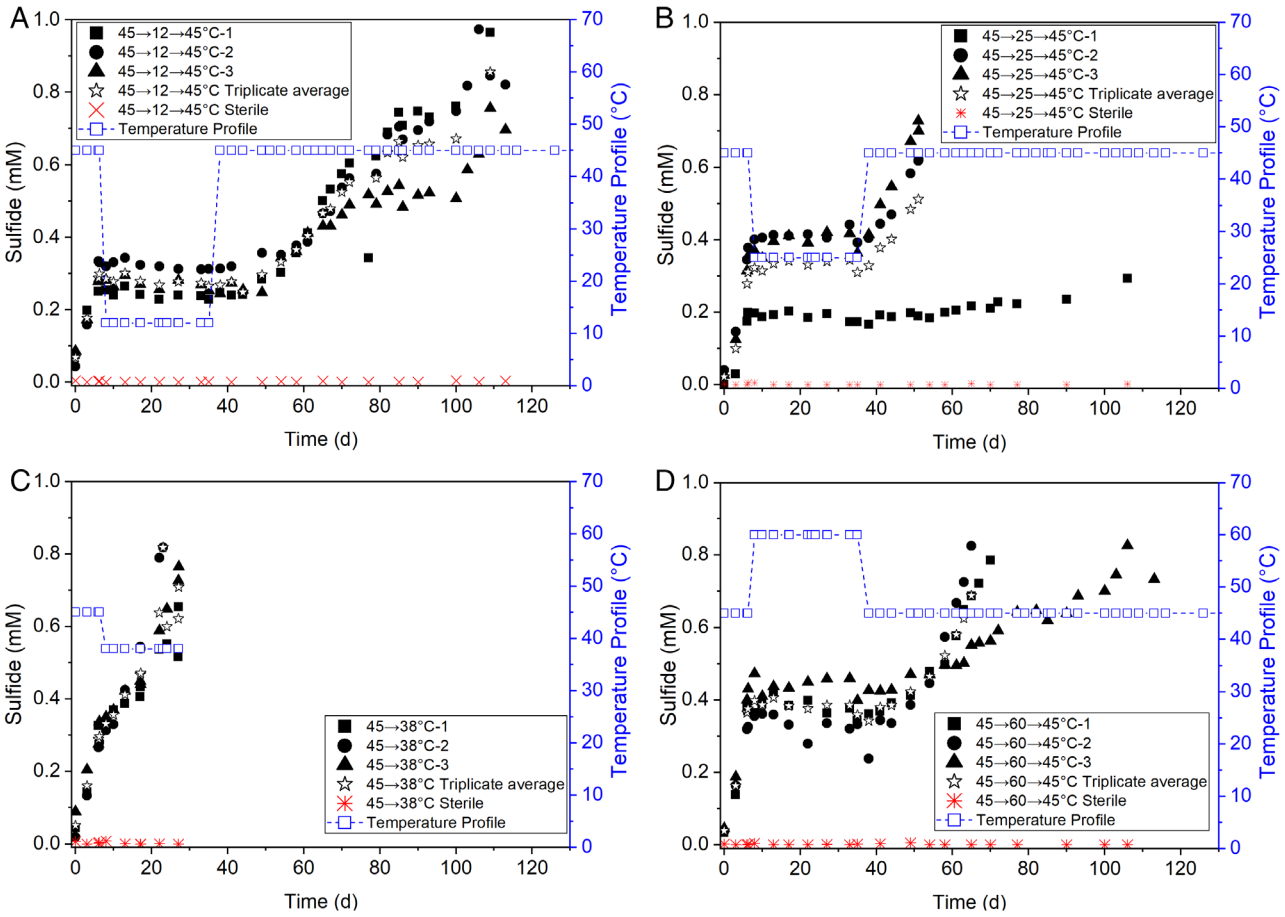

Fig. 3. Time courses on the sulfide production from microcosms in treatments 5 (45 → 12 → 45°C) (A), 6 (45 → 25 → 45°C) (B), 7 (45 → 38°C) (C) and 8 (45 → 60 → 45°C) (D). In treatment 7, the experiment was completed during incubation at 38°C and was not returned to 45°C.

and genus levels (Fig. 4A and B). The communities from treatment 4 (45 → 60°C) could not be sequenced due to insufficient DNA extracted from the biomass. In the community incubated continuously at 45°C, the dominant phylotypes belonged to the orders *Spirochaetales* (~ 56%), *Clostridiales* (~ 30%) and *Bacteroidiales* (9%) (Fig. 4A). At the genus level, members comprised mainly of uncultured members of the *Spirochaetaceae* (~56%) and *Desulfotomaculum* (~ 30%) (Fig. 4B). In replicate 4.07 of treatment 2 (45 → 12°C) sacrificed on day 126, and replicate 4.09 of treatment 3 (45 → 25°C) sacrificed on day 82, the orders *Spirochaetales* and *Clostridiales* were highly abundant as well (Fig. 4A). In treatment 2 (45 → 12°C), the dominant genera were affiliated with uncultured *Spirochaetaceae* (53%) and *Desulfotomaculum* (~ 19%). *Candidatus* Desulforudis (~19%), an uncultured bacterium of *Anaerolineae* (~4%) and *Pelolinea* (~4%) were more abundant in treatment 2, whereas these genera only ranged between 0.9% and 1.5% in treatment 1 (Fig. 4B). In contrast, several abundant phylotypes present in replicate 4.09 of treatment 3 (45 → 25°C) consisted of *Desulfotomaculum* (51%), uncultured *Spirochaetaceae* (21%) and *Symbiobacterium* (17%).

Eight replicates were sacrificed to investigate the community composition at the end of the experiment after the entire cycle of heat exchange (Figs. 5 and S3). In general, all replicates showed a high abundance of *Spirochaetales* (32%–61%) and *Clostridiales* (21%–56%) (Fig. S3). Other phylotypes which were present, albeit in varying abundances, included *Clostridia incertae sedis* (0.7% to ~18%), *Bacillales* (0.5% to ~4%) and *Bacteroidales* (0.01% to ~8%) (Fig. S3). At the genus level, highly abundant phylotypes across the eight replicates were affiliated with *Desulfotomaculum* (~15% to 56%) and *Candidatus* Desulforudis (~0.8% to 18%) besides uncultured relatives of the *Spirochaetales* (Fig. 5). Several other phylotypes that were also present with varying abundances included a *Rikenellaceae* member (0%–8%), *Ruminococcaceae* (0%–9%) and *Ureibacillus* (~1%–4%).

Three replicates were set up for each of treatments S1 (45 → 25 → 45°C) and S2 (45 → 60 → 45°C) to

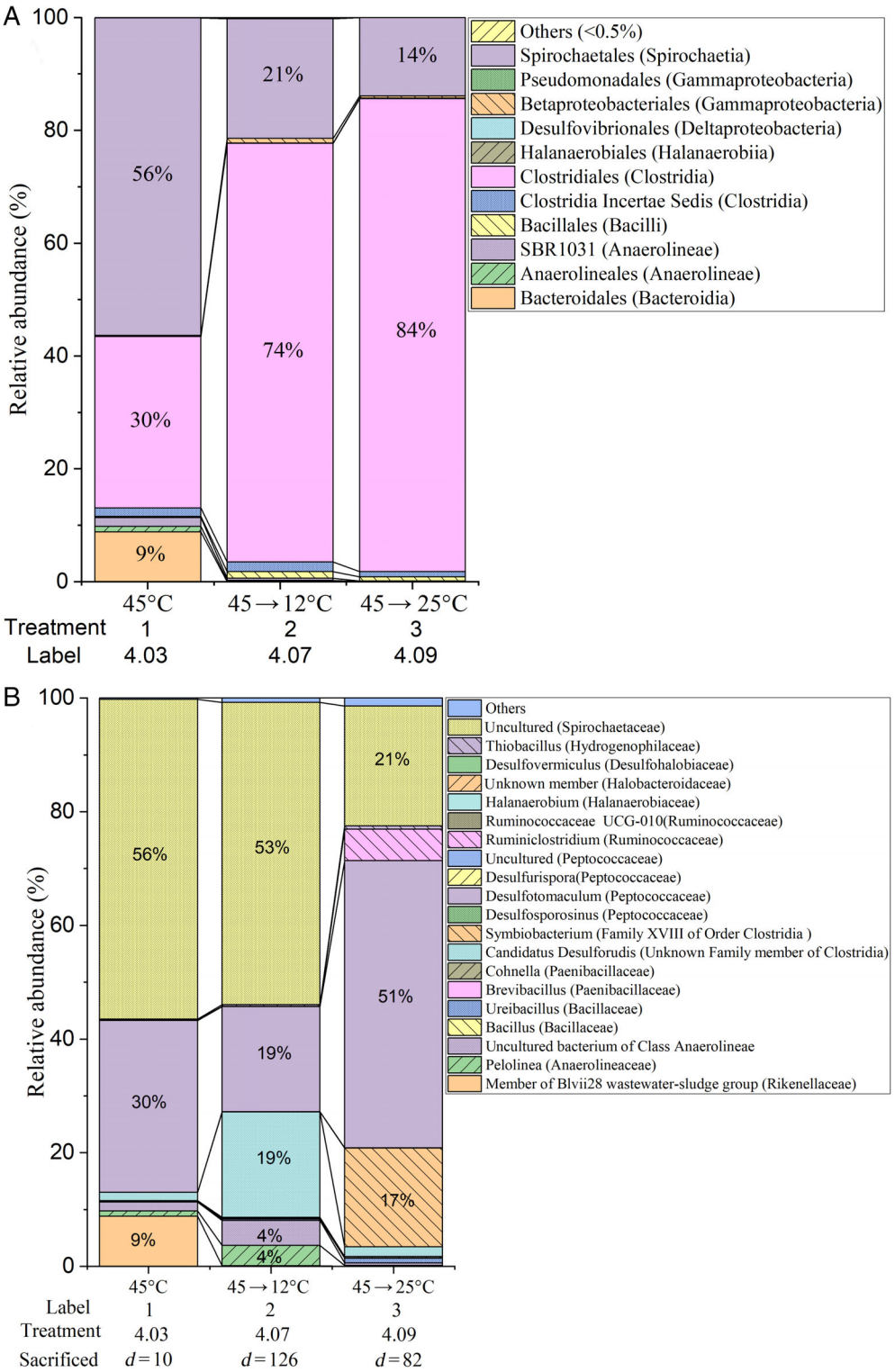

Fig. 4. Microbial community compositions for three treatments: 1 (45°C), 2 (45 → 12°C) and 3 (45 → 25°C), (A) represented at the order level (class level in parentheses), and (B) represented at the genera level (corresponding family level in parentheses). Community composition of treatment 4 (45 → 60°C) could not be obtained due to insufficient biomass.

investigate the community at each stage of the cycle with one replicate sacrificed each for pre-, post-temperature change and finally at the end of the cycle (Table S2). The replicates were monitored for acetate mineralization and sulfide production (Table 3) and behaved similarly as the replicates shown in Figs 3 and 4. Microbial community

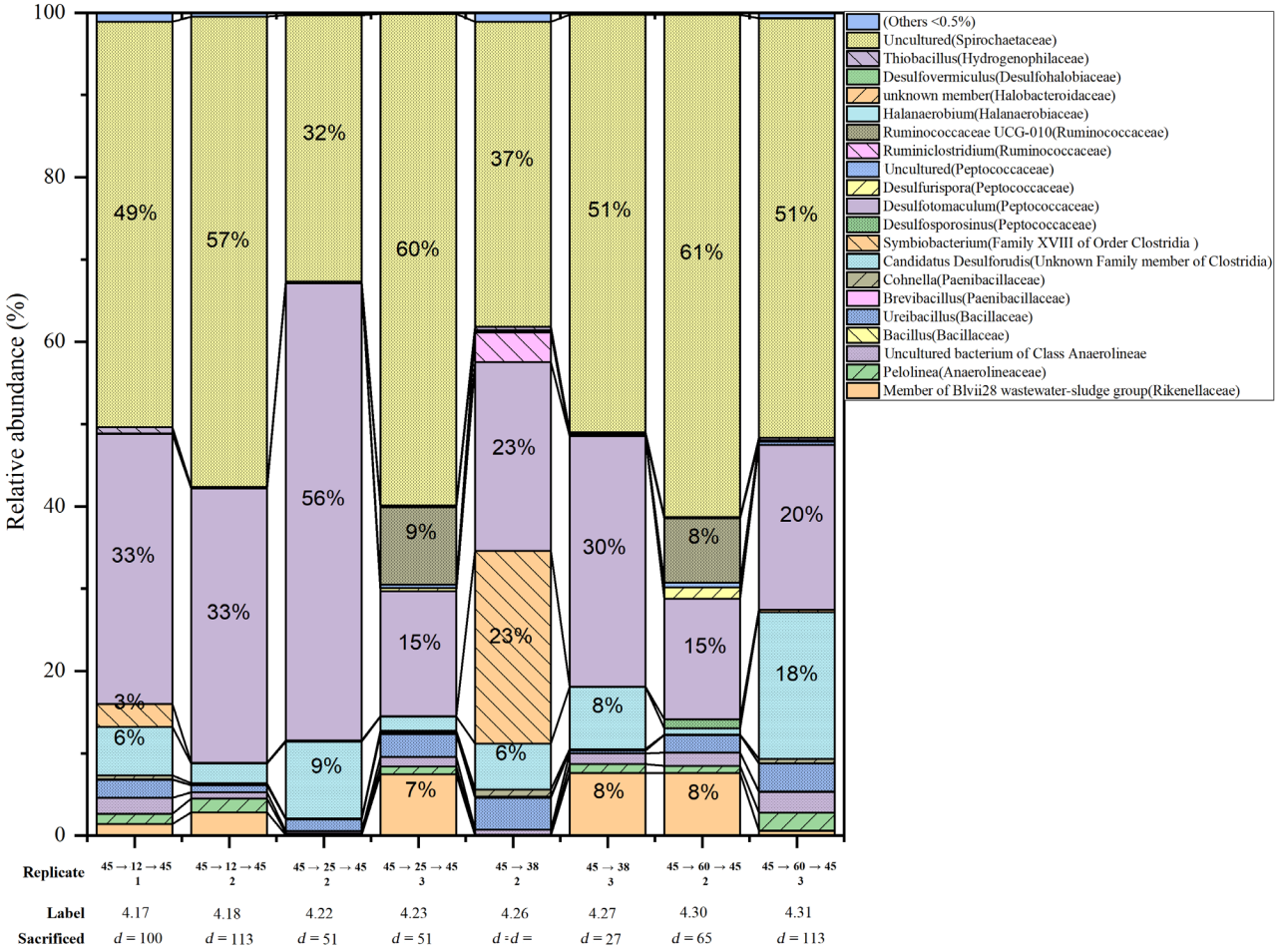

Fig. 5. Microbial community compositions of treatments: 5 (45 → 12 → 45°C), 6 (45 → 25 → 45°C), 7 (45 → 38°C) and 8 (45 → 60 → 45°C), represented at the genera level and the family level in parentheses. 'Replicate' and 'Label' information correspond to the replicate assignment described in Table S2. Two replicates were sacrificed from each treatment: 45 → 12 → 45°C (labels 4.17 and 4.18), 45 → 25 → 45°C (labels 4.22 and 4.23), 45 → 38°C (labels 4.26 and 4.27) and 45 → 60 → 45°C (labels 4.30 and 4.31). For consistency, replicates were numerically assigned (e.g., 45 → 12 → 45°C 1 or 45 → 12 → 45°C 2) corresponding to replicate assignments (Table S2). Two replicates, 4.26 and 4.27 were sacrificed at 38°C as the experiment was completed.

compositions of treatments S1 (45 → 25 → 45°C) and S2 (45 → 60 → 45°C) at genus level are represented in Fig. 6 (for compositions at the order level see Fig. S4). For treatment S1, phylotypes affiliated with uncultured members of the *Spirochaetaceae* (22%–35%) and *Desulfotomaculum* (22%–39%) were the most abundant genera across the three replicates subjected to the 45 → 25 → 45°C cycle. Several phylotypes such as *Pelolinea* (4%) and an uncultured member of the *Anaerolineae* (8%), were initially present at 45°C before temperature change at day 6; however, this diminished to 0.3%–1.1% at the end of the 45 → 25 → 45°C cycle, although *Pelolinea* abundance initially increased to ∼15% in the replicate 4.34 sacrificed after incubation at 25°C (Fig. 6). Meanwhile, *Candidatus* Desulforudis, which had a high relative abundance (∼18%) in replicate 4.35 (pre temperature change), saw a lower abundance (∼2%) in replicate 4.34 sacrificed at the end of the 25°C, which rebounded to ∼6% in replicate 4.33 sacrificed at the end of the 45 → 25 → 45°C cycle. Phylotypes such as *Brevibacillus* and *Bacillus* were initially present in the sacrificed replicate 4.35 ($d = 6$) but were subsequently absent in the replicates 4.34 ($t = 35$ d) and 4.33 ($t = 120$ d), while *Ureibacillus* abundance fluctuated slightly within the three replicates (Fig. 6).

In treatment S2 (45 → 60 → 45°C), phylotypes affiliated with the uncultured member of the *Spirochaetaceae* (38%–59%) and *Desulfotomaculum* (22%–44%) were the most abundant genera across the three replicates. Phylotypes affiliated to the *Rikenellaceae* (∼12%) and *Candidatus* Desulforudis (∼3%) were initially present at 45°C before temperature change at day 6; however, both taxa diminished to ∼1.0% at the end of the 45 → 60 → 45°C cycle. *Candidatus* Desulforudis abundance was however slightly higher (∼5%) in the replicate 4.37 sacrificed post-incubation at 60°C (Fig. 6).

Table 3. Overview on results of six replicates of acetate mineralization, sulfide production and rates for treatments S1 and S2.

Objective		Heat exchange					
	Treatment	S1			S2		
	Batch	45 → 25 → 45°C	45 → 25 → 45°C	45 → 25 → 45°C	45 → 60 → 45°C	45 → 60 → 45°C	45 → 60 → 45°C
	Label	4.35	4.34	4.33	4.38	4.37	4.36
Stage	Stage sacrificed	Pre	Post	End	Pre	Post	End
Pre	Duration (d)	6.25	6.25	6.25	6.25	6.25	6.25
	Acetate mineralized (%)	30.4	13.5	6.5	26.4	16.8	20.9
	Acetate mineralized (μM)	304	135.5	65	264.3	167.5	208.7
	Rate (μM acetate d^{-1})	48.6	21.7	10.4	42.3	26.8	33.4
	Duration (d)	6.25	6.25	6.25	6.25	6.25	6.25
	Sulfide produced (μM)	303	134.4	139.1	274.7	167.2	194
	Rate (μM acetate d^{-1})	48.5	21.5	22.2	44	26.7	31.0
Post	Duration (d)	Sacrificed	28.75	28.75	Sacrificed	28.75	28.75
	Acetate mineralized (%)	-	3.5	5.1	-	1.23[a.]	0.9[a.]
	Acetate mineralized (μM)	-	35	50.6	-	12.4[a.]	9[a.]
	Rate (μM acetate d^{-1})	-	1.2	1.8	-	-	-
	Duration (d)	-	28.75	28.75	-	28.75	28.75
	Sulfide produced (μM)	-	-	-	-	-	-
	Rate (μM sulfide d^{-1})	-	-	-	-	-	-
End	Duration (d)	Sacrificed	Sacrificed	85	Sacrificed	Sacrificed	47
	Acetate mineralized (%)	-	-	60.7	-	-	85.5
	Acetate mineralized (μM)	-	-	607.2	-	-	855.3
	Rate (μM acetate d^{-1})	-	-	7.1	-	-	18.2
	Duration (d)	-	-	81	-	-	47
	Sulfide produced (μM)	-	-	503.2	-	-	569.2
	Rate (μM sulfide d^{-1})	-	-	6.2	-	-	12.1

[a.]Acetate mineralization due to residual activity after shifting to 60°C.

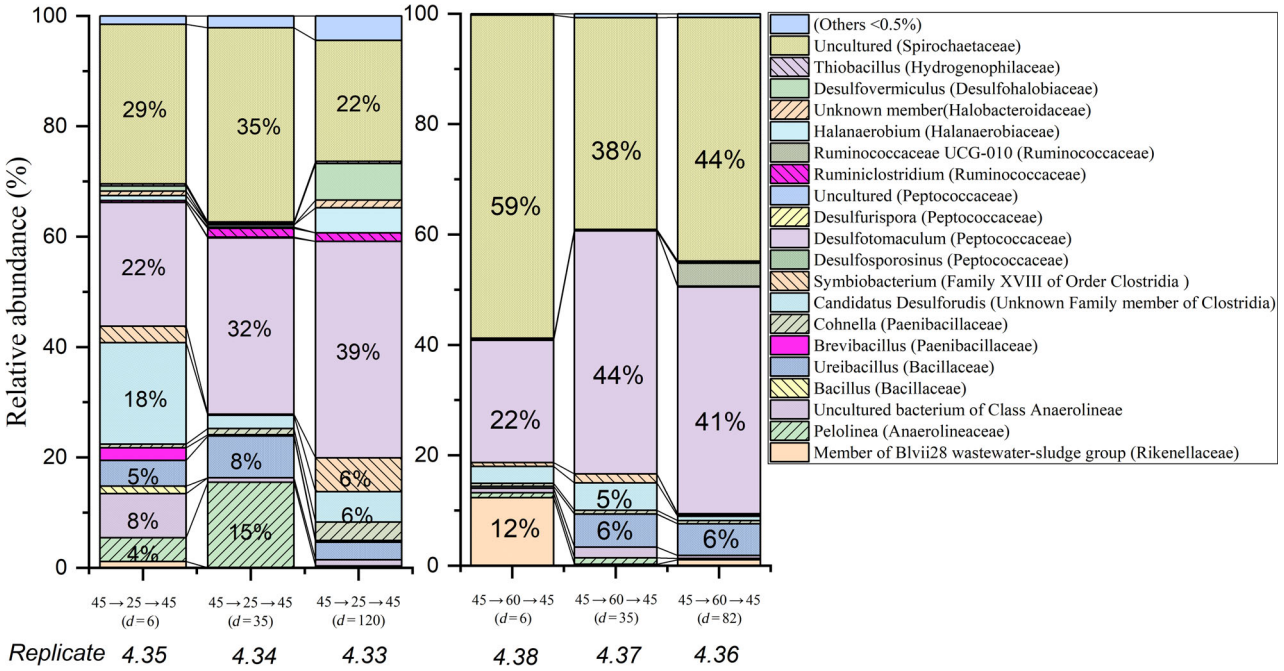

Fig. 6. Microbial community of the replicates sacrificed at various stages of the heat exchange, that is 'Pre' ($d = 6$), 'Post' ($d = 35$) and 'End' of the experiment ($d = 120$ and $d = 82$). Sequences are represented at the genus level, with the family level represented in parenthesis.

Microbial diversity indices of the differently treated communities are provided in Figures S6–S8.

Discussion

This study highlights the sulfate reduction potential of aquifer microbial communities at the boundary between mesophilic and thermophilic conditions. Acetate is a commonly reported intermediate during degradation of organic substrates (Thauer *et al*., 1989), for example in sulfidogenic benzene mineralization (Rakoczy *et al*., 2011; Starke *et al*., 2016), and was therefore used as a model carbon source for studying heterotrophic microbial activity in an aquifer microbial community originally adapted to anaerobic hydrocarbon degradation (Bin Hudari *et al*., 2020). Our data indicate that at 45°C (and also at 38°C, 25°C and 12°C), the bacterial community mineralized acetate with sulfate as the sole electron acceptor due to the ratio of produced sulfide to oxidized acetate of around 1 (Table 1) according to the following equation:

$$CH_3COO^- + SO_4^{2-} \rightarrow 2HCO_3^- + HS^-$$

The sulfide production rate at 45°C (51.8 ± 3.8 μM d^{-1}) was approximately ten times higher compared to a previous study at the same temperature (Bin Hudari *et al*., 2020), illustrating that the enriched consortium was well adapted to 45°C. While sulfate reduction (SR) rates are often reported for typical mesophilic (e.g. 20–38°C) or thermophilic (e.g. 50–70°C) conditions (Isaksen *et al*., 1994; Elsgaard *et al*., 1994a,b; Kallmeyer and Boetius, 2004; Jesußek *et al*., 2012; Frank *et al*., 2015), rates for temperatures in between the meso-thermophilic range (~45°C) are scarce. The determined value for sulfide production d^{-1} in our study is in the range reported for SR rates between 42°C and 50°C ranging between ~25 and 316 μM sulfate d^{-1} (Frank *et al*., 2015; Robador *et al*., 2016). Alongside sulfide and labelled carbon dioxide production, the rate of pre- and post-temperature change reaffirms the impact periodic temperature fluctuations have on biotransformation. Cultures continuously incubated at 45°C were dominated by phylotypes distantly affiliated to the genus *Desulfotomaculum* and an uncultured member of the family *Spirochaetaceae*. *Desulfotomaculum* are sulfate reducers, which have been reported in various settings (Klemps *et al*., 1985; Bak and Pfennig, 1991; Aullo *et al*., 2013; Bonte *et al*., 2013; O'Sullivan *et al*., 2015; Tian *et al*., 2017). They are endospore formers (Widdel and Bak, 2006; Aullo *et al*., 2013; O'Sullivan *et al*., 2015; Grigoryan *et al*., 2018) and have been described at various temperatures including psychrophilic and thermophilic conditions (Klemps *et al*., 1985; Widdel and Bak, 2006; Aullo *et al*., 2013; O'Sullivan *et al*., 2015), thus, their higher

abundance at 45°C is not a surprise, and they are believed to oxidize acetate in our 45°C community, since several species such as *D. acetoxidans* and *D. kuznetsovii* are capable of utilizing acetate under sulfate-reducing conditions (Widdel and Pfennig, 1977; Thauer *et al*., 1989; O'Sullivan *et al*., 2015). However, the phylotype enriched in our 45°C culture was not clearly affiliated to known acetate mineralizing species of *Desulfotomaculum*, indicating that novel acetate-mineralizing *Desulfotomaculum* phylotypes could be responsible for the acetate-driven sulfate reduction at 45°C. A BLAST analysis of the 16S rRNA gene sequences (Table S4) revealed that the phylotype was affiliated to an uncultured *Sporotomaculum* sp. (99.8%) and to *Desulfallas thermosapovorans* DSM 6562 (98.5%) as closest relatives (Table S4). *Sporotomaculum* have been reported in setups with acetate as an electron donor under sulfate reducing conditions, but species reported from this genus are not known to be sulfate reducers (Brauman *et al*., 1998; Qiu *et al*., 2003; Purkamo *et al*., 2017; Hessler *et al*., 2020). Unlike *Sporotomaculum*, strains of *D. thermosapovorans* are sulfate reducers and with an optimal growth temperature of 50°C; however, they have not been described yet as acetate oxidizers (Fardeau *et al*., 1995). Meanwhile, the consistently high abundance of *Spirochaetaceae* across the 18 replicates (21%–61%) demonstrates they grew under the selected conditions. Although *Spirochaetaceae* have often been observed in anoxic habitats including sulfate-reducing conditions (Magot *et al*., 1997; Muller *et al*., 2009; Baldwin *et al*., 2016; Saad *et al*., 2017; Zouch *et al*., 2017; Dong *et al*., 2018; Bratkova *et al*., 2019; Bin Hudari *et al*., 2020; Ozuolmez *et al*., 2020; Yi *et al*., 2020), the capability for dissimilatory sulfate reduction has not been demonstrated in this family yet. In a naphthalene-degrading sulfate-reducing consortium, it was shown that a phylotype belonging to the *Spirochaetales* was recycling necromass by fermenting carbohydrates and proteins released from dead cells of the sulfate reducer and thereby producing hydrogen usable by the sulfate reducers (Koelschbach *et al*., 2017; Saad *et al*., 2017; Dong *et al*., 2018), and we assume therefore that necromass cycling was the main lifestyle of *Spirochaetaceae* in our enriched communities. Meanwhile, based on this study, there does not seem to be other predominant putative necromass recyclers capable of growth at 45°C, which implies that this phylotype is well suited for the mesophilic-thermophilic boundary (45°C) at anoxic conditions.

The key organisms in the 45°C consortium seem to be adapted to temperatures lying in the upper mesophilic to lower thermophilic zone. Some acetate mineralizers, *D. acetoxidans and D. thermoacetoxidans*, have an optimum growth temperature of 34–36°C (range: 20–40°C) and 55–60°C (range: 45–65°C) respectively (Min and Zinder, 1990; Stackebrandt *et al*., 1997; Widdel and Bak, 2006). Other sulfate reducers adapted to around 45°C that have not yet been shown to oxidize acetate are *D. geothermicum and D. sapomendans* with optimum temperatures of 54°C (range: 37–56°C) and 38°C (range: 20–43°C) respectively (Cord-Ruwisch and Garcia, 1985; Daumas *et al*., 1988; Widdel and Bak, 2006). Several *Anaerolineae* species were also reported to grow within the 25–60°C range, for example *Levilinea saccharolytica* KIBI-1 (optimum: 37°C, range: 25–50°C) and *Anaerolinea thermolimosa* IMO-1T (optimum: 50°C, range: 42–55°C) (Imachi *et al*., 2014). However, it is important to note that *Anaerolineae* were not particularly dominant in this study as compared to our earlier study where phylotypes belonging to this group were found to be dominant at 45°C under sulfate-reducing conditions (Bin Hudari *et al*., 2020), indicating that endospore-forming sulfate reducers and *Spirochaetaceae* are outcompeting *Anaerolineae* phylotypes after prolonged batch incubation at 45°C using acetate and sulfate as main carbon substrate and electron acceptor.

When exposed to a new temperature, a sustained mineralization of dissolved organic carbons (including pollutants) might be possible by either a succession of the microbial community resulting in the bloom of novel, temperature-adapted species occupying the same ecological niche, or by a temperature-specific intracellular adaptation of key species (Ranneklev and Baath, 2001; Delille *et al*., 2004). The latter is rather unlikely for broader temperature changes as prokaryotes are usually active in a temperature window of around Δ25°C (Madigan *et al*., 2017; see also discussion below). Hence, the observed resumption of activity at 12°C and 25°C can be best explained by a resilience of the original community to prolonged incubation at 45°C. However, the sequencing data did not clearly indicate a putative acetate oxidizer exclusively becoming enriched at 12°C or 25°C. Notably, the Desulfotomaculum phylotype, which is one of the putative key acetate degraders at 45°C and may be related to *Desulfallas thermosapovorans* (Table S4), was still abundant after mineralization of acetate at 12°C and 25°C (Fig. 4B); the relative abundance of this phylotype in treatment 3 (∼51%; 45 → 25°C) was also higher than in replicates of treatments 2 (∼19%; 45 → 12°C) and 1 (∼30%) incubated continuously at 45°C. One particular observation with respect to the community at the end of treatment 2 (45 → 12°C) was the higher abundance (∼19%) – compared to the setup incubated solely at 45°C – of a phylotype distantly related to *Candidatus* Desulforudis (Fig. 4). Only one species has been affiliated to *Candidatus* Desulforudis thus far, *Candidatus* Desulforudis audaxviator (∼93.0% identity, Table S4), which is

endospore forming and sulfate reducing (Jungbluth *et al*., 2017). *Candidatus* Desulforudis audaxviator was reported to grow between 45°C and 60°C with an optimal growth temperature of 55°C; however, it cannot grow with acetate (Karnachuk *et al*., 2019). In view of the relatively low percentage of identity, the enriched phylotype might be a new species of the genus *Candidatus* Desulforudis. This phylotype was also enriched at the end of incubation in the approaches 45-60-45, 45-38 and 45-25-45 (Fig. 5), pointing to an active role at 38–45°C rather than 12°C and 25°C. It is worth noting that since both phylotypes affiliated to *Desulfallas* and *Candidatus* Desulforudis were present in most of the treatments (Table S4), albeit at different relative abundances, we cannot exclude *per se* that both phylotypes were also active at 12°C and 25°C. Thus, the amplicon sequencing approach was not sensitive enough to differentiate between putative temperature-adapted subtypes. Other than that, the endospore survival strategy of both *Desulfotomaculum* and *Candidatus* Desulforudis could also have contributed to these phylotypes becoming more dominant at 45°C and staying dominant (at 45°C) even after the subsequent temperature changes in treatments 5 (45 → 12 → 45°C), 6 (45 → 25 → 45°C) and 8 (45 → 60 → 45°C). Notably, a phlyotype affiliated to the genus *Symbiobacterium* was abundant in two communities after longer incubation at 25°C (17%; treatment 3, Fig. 4) and 38°C (23%; treatment 7, Fig. 5), indicating an active role of this organisms for acetate oxidation at mesophilic conditions. *Symbiobacterium* is not known for sulfate reduction but has been identified to oxidize acetate syntrophically (Liu and Conrad, 2010).

In a previous study done by our group using an inoculum incubated for several years at room temperature (~ 20°C), completely different communities as well as sulfate reducers were identified (Bin Hudari *et al*., 2020). For example, several putative sulfate-reducing phylotypes related to *Desulfoprunum*, *Desulfovibrio* and *Desulfurivibrio* were present and more abundant in the 12°C and 25°C incubations while the *Desulfatiglans* and *Desufurivibrio* were present but in consistently lower abundances at 38°C (Bin Hudari *et al*., 2020). Sulfate reducers of the endospore-forming order Clostridia (e.g., *Desulfotomaculum*) were present in these setups but in markedly lower abundances (Bin Hudari *et al*., 2020). The considerable differences in the communities particularly the phylogenies of putative sulfate reducers in relation to this study further highlight the role of temperature in the succession of the native community.

Nevertheless, 45°C was the upper limit for acetate mineralization and sulfide production in our investigated community and within the experimental set up, and therefore thermophilic acetate degraders nor thermophilic sulfate reducers were probably not present, or present in such low numbers that the incubation time of this study was not long enough to detect their activity. However, active anaerobic thermophiles have been reported in aquifer sediments at 60°C (Bonte *et al*., 2013; Karnachuk *et al*., 2019), as well as aerobic thermophiles which seem to be more abundant in subsurface microbial communities (Metze *et al*., 2021; Bin Hudari *et al*., 2020). Therefore, the question regarding the ubiquity of especially anaerobic thermophiles in shallow aquifer sediments needs to be explored in future (long term) studies.

Implications and outlook

To our knowledge, very few ATES-related studies have reported adaptation or recovery following periodic incubation at higher (heat storage) or lower temperatures (cold storage). From the ATES standpoint, 45°C is above that of the typical ATES threshold (~25°C) in Europe. However, this is considered to be a relevant temperature in HT-ATES systems, either in the operational space (the water that is usually extracted within the inner space of the system) in case of added heat up to 50°C, or in the outer, affected space in case of higher temperatures (above 60°C) in the operational space (Lerm *et al*., 2013; Kallesøe and Vangkilde-Pedersen, 2019). Our data indicate that natural aquifer communities harbor organisms well adapted to temperatures of the overlapping mesophilic-thermophilic boundary, sustaining the carbon cycle and being resilient to temperature fluctuations; overall, microbial activity could be sustained or resumed under the different temperature settings. This key finding indicates that cold storage (injection of cooler water during winter) or heat storage (injection of warmer water) ATES installations will change the structure of microbial communities but will not generally disturb microbial ecosystem services. However, the ultimate target remains to assess the feasibility of HT-ATES, using temperatures above, for example 60°C that would select for thermophilic or hyperthermophilic species. Our results suggest that above 60°C only a few (if any) thermophiles will be active in the operational space of a HT-ATES system. On the other hand, truly thermophilic communities may evolve at long-term operation of HT-ATES systems; especially at anoxic conditions, growth rates are usually low and a small inoculum of thermophilic initial community members may need several months or even years to considerably enrich. Additionally, inocula are probably site dependent, relying on a suitable microbial consortium to carry out biotransformations (Kallmeyer and Boetius, 2004). For example, communities isolated or well adapted in temperatures of up to 80°C have been described in in oil reservoirs of the deep subsurface, with the ability to degrade hydrocarbons (Head *et al*., 2014;

Piceno *et al*., 2014; Tian *et al*., 2017). However, it is unclear if these thermophilic organisms are present (albeit at very low numbers) in shallower aquifers and will only develop after a certain lag phase. Therefore, more studies utilizing different sediments are still required to investigate community resilience in the mesophilic-thermophilic boundary.

A higher threshold for LT-ATES to allow larger thermal energy storage while simultaneously remediating contaminants would be advantageous. Additionally, a more optimistic scenario of HT-ATES is where the society accepts that although the operational space of HT-ATES systems is being 'a microbial desert' and characterized by reduced or absent microbial activity, the (much bigger and less heated) affected space still contains active microbial communities which can perform ecosystem services. There is still some uncertainty how HT-ATES or higher threshold LT-ATES (~45°C, this study) could be maintained in the long term, where knowledge on community resilience and thermal cycling fatigue is still limited. The seasonal mode of ATES operations can cause fluctuations in the subsurface (Saito *et al*., 2016); therefore, the impacts of repeated heat exchange cycling at higher temperature thresholds need to be addressed. Furthermore, the effects of periodic heat exchange on nutrient availability and physicochemical characteristics of the contaminants should also be studied (Head *et al*., 2014). For example, an increase in temperature can result in lower organic carbon, total nitrogen or phosphorus (Jiao *et al*., 2016), while in others warming resulted in increases in carbon, total nitrogen and phosphorus (Geng *et al*., 2017; Gong *et al*., 2019). Understanding the overall impact of periodic heat exchange is an important step towards the goal of raising thermal storage thresholds. Multiple heat cycle experiments, combined with different heat exchange scenarios coupled with stable isotope probing, could also be applied to understand the long term effects of HT-ATES on ecosystem services and bioremediation.

Experimental procedures

Chemicals

Chemicals used were purchased from Sigma-Aldrich (USA), Merck (Germany) and Carl Roth (Germany) unless stated otherwise. Uniformly ^{13}C-labelled sodium acetate was purchased from Cambridge Isotope Laboratories (98% purity, 99 atom %, Massachusetts, USA).

Experimental setup

The inoculum used in this study belonged to an acetate-mineralizing sulfate-reducing enrichment culture (Zox4) consolidated from microbial communities of two microcosms (Zz-O1 and Zz-O2) comprising coarse sand obtained from the columns of an *on-site* system percolated with sulfidic benzene-contaminated groundwater, which were in operation for up to 10 years and 6 months at a mean temperature of 15°C as described elsewhere (Vogt *et al*., 2007; Taubert *et al*., 2012). The site, located north of the city of Zeitz in Central Germany, is contaminated for several decades by hydrocarbons and benzene due to former operations by an hydrogenation plant during world war II, and a benzene production plant between 1965 and 1990 (Schirmer *et al*., 2006). Zz-O1 and Zz-O2 were incubated since June 2010 at room temperature at sulfate-reducing conditions using benzene as substrate. Zz-O1 and Zz-O2 were believed to be slightly exposed to oxygen based on the presence of a lighter upper layer formed in the coarse sand with respect to the darker layer (Fig. S1). For preparing acetate-mineralizing enrichment cultures, the light, oxidized layers were removed from both Zz-O1 and Zz-O2 bottles and the dark, anoxic layers were distributed into six 0.5 l Schott bottles (Fig. S5) and filled with anoxic bicarbonate-buffered mineral salt medium (Bak and Pfennig, 1991) comprising 10 mM sulfate as electron acceptor and supplemented with 2 mM acetate as the electron donor (see Table S1 for composition). The new enrichment cultures were each placed at different incubation temperatures: 12°C, 25°C, 38°C, 45°C, 60°C and 80°C (labelled as Zox1, 2, 3, 4, 5, and 6 respectively), and monitored for sulfide production as an indicator for sulfate reduction activity (Fig. S5). Only cultures Zox1-4 (corresponding to 12°C, 25°C, 38°C, 45°C) produced sulfide (results not shown). For this study, the coarse sand of Zox4, which was enriched at 45°C for about 310 days, was used as an inoculum to set up 35 replicate bottles (Fig. S5); details of the replicate assignments can be found in Table S2. All replicates were prepared in 120 ml serum flasks made up of 5 g (treatments 1–8) or 15 g (treatments S1 and S2) coarse sand, and filled with 80 ml of modified carbonate-buffered mineral salt medium (Bak and Pfennig, 1991; see Table S1 for composition) amended with 10 mM sulfate and gas-tight sealed with Teflon-coated butyl rubber stoppers (Wheaton Industries, USA) and crimped aluminum caps. Treatment 1 served as 45°C reference (4.01 to 4.04 in Fig. S5) comprising three biotic replicates and one replicate (4.04) which was sterilized. In the 'adaptation' scenario, a total of nine biotic replicates were evenly distributed and firstly incubated at 45°C for 6 days before being transferred to 12°C for a further 120–127 days (treatment 2), to 25°C for up to 100 days (treatment 3) or to 60°C for 100 days (treatment 4) (4.05–4.15 in Fig. S5). Thus, an exception was made for treatment 2 (45 → 12°C) for additional incubation time, when mineralization commenced after $t = 70$ d allowing mineralization and sulfide

production to proceed (Fig. 1C and D). For the 'heat exchange' scenario, four replicates (three biotic and one sterilized) were each first incubated at 45°C for 6 days, followed by a periodic incubation for 28 days at 12°C (treatment 5), 25°C (treatment 6), 38°C (treatment 7) or 60°C (treatment 8), and finally returned to 45°C on $t = 35$ d for up to 78 days (4.17–4.32, Fig. S5). Replicates of treatments 1–8 were regularly sampled for sulfide and $\delta^{13}CO_2$ analyses; in some of the replicates, the microbial community was analysed at the end of the experiment (Fig. S5, Table S2A). Another six biotic replicates (4.33–4.38, Fig. S5) were set up for microbial community analysis at distinct time points of incubation using the entire bottle content ('phased sacrifice', Table S2B). Three replicates were assigned to each of treatments S1 (45 → 25 → 45°C) and S2 (45 → 60 → 45°C) to analyse community composition at different stages of the heat exchange (Pre, Post and End). For these treatments (S1 and S2), the first replicate was sacrificed at the end of the first incubation period (45°C, $t = 6$ d), the second at the end of the second temperature period (25°C or 60°C, $t = 35$ d, termed 'after') and the third at the end of the third temperature period (45°C, $t = 120$ d for replicate 4.33 and $t = 82$ d for replicate 4.36). Sulfide concentrations and $\delta^{13}CO_2$ values were analysed for each of the replicates.

Sterile controls were set up by autoclaving microcosms prepared as described above three times at 121°C for 20 min on three consecutive days. Prior to amendment of ^{13}C-labelled acetate (see below), microcosms were incubated at 45°C for three days to allow microcosms to thermally acclimatize. Uniformly ^{13}C-labelled sodium acetate from a sterile anoxic stock solution (100 mM) was added to each microcosm via a plastic syringe (B Braun, Germany) to a final concentration of 1 mM. Microcosms were incubated horizontally and statically in the dark at 12°C, 25°C, 38°C, 45°C or 60°C using different incubators (IN55, Memmert, Germany; Heraeus incubator, Thermoscience, USA). All used glassware was sterilized by autoclaving (121°C, 20 min) before usage. Microcosms were prepared in an anaerobic glove box (97% N_2 / 3% H_2 gas atmosphere, Coy Laboratory Products, USA) to avoid contamination by oxygen.

Chemical analyses

Analysis of $\delta^{13}CO_2$. Headspace samples (4 ml) were collected during the course of the experiment in N_2-flushed (2 min, 1 bar) glass vials (10 ml) via N_2-flushed syringes, which were crimped-sealed with Teflon-coated butyl rubber stoppers. Carbon isotope ratios of carbon dioxide for headspace CO_2 and CH_4 were measured by gas chromatography-combustion-isotopic ratio mass spectrometer (GC-IRMS) as described elsewhere (Bin Hudari *et al*., 2020).

The percent of mineralization (MIN %) of each replicate was calculated according to the following equation (Dorer *et al*., 2016):

$$\mathrm{MIN}\,(\%) = \frac{\left[\mathrm{HCO_3^-}\right] \times R_{\mathrm{VPDB}} \times (\delta_{\mathrm{end}} - \delta_{\mathrm{start}})}{(n-x) \times [\mathrm{acetate}] \times (1 + R_{\mathrm{VPDB}} \times (1 + \delta_{\mathrm{start}}))} \times 100 \quad (1)$$

Equation 1 includes isotope values (‰) of both the starting (δ_{start}) and end-point (δ_{end}), the concentrations of bicarbonate (HCO_3^-) and acetate as well as number of labelled carbon atoms of the target compound. The variables n and x represent the total and unlabelled carbon in the substrate respectively, where in the case of fully labelled acetate, $n - x = 2$. This value was used to compare the extent of acetate mineralization between treatments.

Analysis of sulfide. Sulfide was quantified in liquid samples using the modified methylene blue method originally described elsewhere (Cline, 1969; Muller *et al*., 2009). Up to 200 µl of samples were collected over the course of experiment, and samples were prepared as described in detail elsewhere (Bin Hudari *et al*., 2020). Calibration was carried out using a sodium sulfide nonahydrate stock solution (5 mM, Sigma-Aldrich, USA) made by dissolving it in 0.5 l of MilliQ spiked with one NaOH pellet (Carl-Roth, Germany) and flushed with nitrogen.

Microbial community analysis

Selected microcosms were sacrificed over time from each treatment temperature (Fig. S5, Tables S2A and S2B). Briefly, in treatments 1–8, one or two replicates were sacrificed at the end of the experiment. In treatments S1 and S2, one replicate was sacrificed for each of the pre, after and end stage of the heat exchange experiment (Fig. S5, Table S2B). Sessile cells were harvested from the coarse sand material via a series of sodium tetrapyrophosphate treatments using a modified method described elsewhere (Velji and Albright, 1984). First, 0.6 ml of sterile, cold 1% sodium tetrapyrophosphate (Sigma–Aldrich, USA) was added to each microcosm to a final concentration of approximately 0.01% (v/v) and sonicated for three pulses at 10 s each in an ice-water sonicating bath (Bandelin, Germany). The liquid was then transferred into new 50 ml Falcon tubes. This step was repeated for a further three times on the coarse sand: two rounds of sonication with 5 ml of 1% sodium tetrapyrophosphate for three pulses of 20 s each followed by a final round of sonication with 5 ml of 1% sodium tetrapyrophosphate

for one min. After each sonication round, the liquid was consolidated into the Falcon tubes and kept cool in an ice bath. At the end of the sonication step, the Falcon tubes with the consolidated liquid portions were centrifuged at 11000 r.p.m. at 4°C (Type 5804R, Eppendorf, Germany). The supernatant was discarded and the pellet was stored at −38°C in the freezer until DNA extraction. DNA was extracted from thawed cell-sand debris pellets using the DNeasy PowerSoil Kit (Qiagen, Hilden, Germany) as per the manufacturer's instructions and eluted in 30 µl of elution buffer. Extracted DNA was quantified with the Qubit HS (High Sensitivity) Assay kit (Thermo Fisher Scientific, USA) on the Qubit 3.0 Fluorometer (Life Technologies, Malaysia).

Procedures for MiSeq sequencing were similar to a study described elsewhere (Bin Hudari *et al*., 2020) using the same Klindworth primer pair (S-D-Bact-0341-b-S-17/ S-D-Bact-0785-a-A-21).

Sequencing libraries were assembled as described elsewhere using the Illumina MiSeq Reagent Kit v3 (2 x 300 bp) according to manufacturer recommendations on 16S Metagenomic Sequencing Library Preparations (Illumina, 2013) and sequenced on an Illumina Miseq platform at the Department of Environmental Microbiology of the Helmholtz Centre for Environmental Research -UFZ. Analysis of the sequences is similarly to that described by Bin Hudari *et al*. (2020) using QIIME 2 v2019.1 (Bolyen *et al*., 2019) with a pipeline provided by Dr. Denny Popp (UFZ, Department of Environmental Microbiology, Systems Biology of Microbial Communities Working Group). This includes first removing the primer sequences and adapters from the demultiplexed sequences, before trimming and denoising to remove low quality reads and chimeras before being merged. Amplicon sequence variants (ASVs) were assigned to the bacterial DNA against the silva132 database (Quast *et al*., 2013; Yilmaz *et al*., 2014). For analysis of Bray–Curtis dissimilarity and diversity analyses, samples were first rarefied to the minimum sequencing read with minor losses to the total amplicon sequencing variants ASVs (Fig. S2). Sequences were deposited at the European Nucleotide Archive (ENA) under the primary accession number PRJEB46801.

Acknowledgements

The authors acknowledge the support of the Federal Ministry for Economic Affairs and Energy (BMWi) within the funding initiative 'Energiespeicher', project ANGUS II, Grant Number 03ET6122B. The authors further thank Dr. Denny Popp for providing the QIIME 2 pipeline support, Stephan Schreiber for sequencing support and Ines Mausezahl for qPCR facility support.

References

Aullo, T., Ranchou-Peyruse, A., Ollivier, B., and Magot, M. (2013) Desulfotomaculum spp. and related gram-positive sulfate-reducing bacteria in deep subsurface environments. *Front Microbiol* **4**: 362.

Bak, F., and Pfennig, N. (1991) Sulfate-reducing bacteria in littoral sediment of Lake Constance. *FEMS Microbiol Lett* **85**: 43–52.

Baldwin, S., Mattes, A., Rezadehbashi, M., and Taylor, J. (2016) Seasonal microbial population shifts in a bioremediation system treating metal and sulfate-rich seepage. *Minerals* **6**: 36:1–36:17.

Bin Hudari, M.S., Vogt, C., and Richnow, H.H. (2020) Effect of temperature on acetate mineralization kinetics and microbial community composition in a hydrocarbon-affected microbial community during a shift from oxic to sulfidogenic conditions. *Front Microbiol* **11**: 3183.

Bolyen, E., Rideout, J.R., Dillon, M.R., Bokulich, N.A., Abnet, C.C., Al-Ghalith, G.A., *et al*. (2019) Reproducible, interactive, scalable and extensible microbiome data science using QIIME 2. *Nat Biotechnol* **37**: 852–857.

Bonte, M., Roling, W.F., Zaura, E., van der Wielen, P.W., Stuyfzand, P.J., and van Breukelen, B.M. (2013) Impacts of shallow geothermal energy production on redox processes and microbial communities. *Environ Sci Technol* **47**: 14476–14484.

Bratkova, S., Alexieva, Z., Angelov, A., Nikolova, K., Genova, P., Ivanov, R., *et al*. (2019) Efficiency of microbial fuel cells based on the sulfate reduction by lactate and glucose. *Int J Environ Sci Technol* **16**: 6145–6156.

Brauman, A., Müller, J.A., Garcia, J.L., Brune, A., and Schink, B. (1998) Fermentative degradation of 3-hydroxybenzoate in pure culture by a novel strictly anaerobic bacterium, *Sporotomaculum hydroxybenzoicum* gen. nov., sp. nov. *Int J Syst Evol Microbiol* **48**: 215–221.

Cline, J.D. (1969) Spectrophotometric determination of hydrogen sulfide in natural waters 1. *Limnol Oceanogr* **14**: 454–458.

Cord-Ruwisch, R., and Garcia, J.L. (1985) Isolation and characterization of an anaerobic benzoate-degrading spore-forming sulfate-reducing bacterium, *Desulfotomaculum sapomandens* sp. nov. *FEMS Microbiol Lett* **29**: 325–330.

Da Silva, M.L., and Alvarez, P.J. (2004) Enhanced anaerobic biodegradation of benzene-toluene-ethylbenzene-xylene-ethanol mixtures in bioaugmented aquifer columns. *Appl Environ Microbiol* **70**: 4720–4726.

Daumas, S., Cord-Ruwisch, R., and Garcia, J.L. (1988) Desulfotomaculum geothermicum sp. nov., a thermophilic, fatty acid-degrading, sulfate-reducing bacterium isolated with H 2 from geothermal ground water. *Ant Leeuw* **54**: 165–178.

Deeb, R.A., and Alvarez-Cohen, L. (1999) Temperature effects and substrate interactions during the aerobic biotransformation of BTEX mixtures by toluene-enriched consortia and *Rhodococcus rhodochrous*. *Biotechnol Bioeng* **62**: 526–536.

Delille, D., Coulon, F., and Pelletier, E. (2004) Effects of temperature warming during a bioremediation study of natural and nutrient-amended hydrocarbon-contaminated sub-Antarctic soils. *Cold Reg Sci Technol* **40**: 61–70.

Dettmer, K. (2002). "A discussion of the effects of thermal remediation treatments on microbial degradation processes", (ed.) Office of Solid Waste and Emergency Response. URL https://clu-in.org/download/techdrct/dettmer.pdf

Dong, X., Greening, C., Bruls, T., Conrad, R., Guo, K., Blaskowski, S., *et al*. (2018) Fermentative Spirochaetes mediate necromass recycling in anoxic hydrocarbon-contaminated habitats. *ISME J* **12**: 2039–2050.

Dorer, C., Vogt, C., Neu, T.R., Stryhanyuk, H., and Richnow, H.H. (2016) Characterization of toluene and ethylbenzene biodegradation under nitrate-, iron(III)- and manganese(IV)-reducing conditions by compound-specific isotope analysis. *Environ Pollut* **211**: 271–281.

Elsgaard, L., Isaksen, M.F., Jørgensen, B.B., Alayse, A.M., and Jannasch, H.W. (1994a) Microbial sulfate reduction in deep-sea sediments at the Guaymas Basin hydrothermal vent area: influence of temperature and substrates. *Geochim Cosmochim Ac* **58**: 3335–3343.

Elsgaard, L., Prieur, D., Mukwaya, G.M., and Jørgensen, B. B. (1994b) Thermophilic sulfate reduction in hydrothermal sediment of Lake Tanganyika, East Africa. *Appl Environ Microbiol* **60**: 1473–1480.

Elsland, R., Fleiter, T., Jakob, M., Reiter, U., Harmsen, R. and Mines, P. *et al.* (2017). "Heating and Cooling (facts and figures) – the Transformation towards a low-carbon Heating and Cooling sector". URL https://www.isi.fraunhofer.de/content/dam/isi/dokumente/cce/2017/29882_Brochure_Heating-and-Cooling_web.pdf

Fardeau, M.L., Ollivier, B., Patel, B.K., Dwivedi, P., Ragot, M., and Garcia, J.L. (1995) Isolation and characterization of a thermophilic sulfate-reducing bacterium, *Desulfotomaculum thermosapovorans* sp. nov. *Int J Syst Evol Microbiol* **45**: 218–221.

Fleuchaus, P., Godschalk, B., Stober, I., and Blum, P. (2018) Worldwide application of aquifer thermal energy storage – A review. *Renew Sustain Energy Rev* **94**: 861–876.

Fleuchaus, P., Schüppler, S., Bloemendal, M., Guglielmetti, L., Opel, O., and Blum, P. (2020) Risk analysis of high-temperature aquifer thermal energy storage (HT-ATES). *Renew Sustain Energy Rev* **133**: p110153.

Frank, K.L., Rogers, K.L., Rogers, D.R., Johnston, D.T., and Girguis, P.R. (2015) Key factors influencing rates of heterotrophic sulfate reduction in active seafloor hydrothermal massive sulfide deposits. *Front Microbiol* **6**: 1449.

Friis, A.K., Edwards, E.A., Albrechtsen, H.J., Udell, K.S., Duhamel, M., and Bjerg, P.L. (2007a) Dechlorination after thermal treatment of a TCE-contaminated aquifer: laboratory experiments. *Chemosphere* **67**: 816–825.

Friis, A.K., Heimann, A.C., Jakobsen, R., Albrechtsen, H.J., Cox, E., and Bjerg, P.L. (2007b) Temperature dependence of anaerobic TCE-dechlorination in a highly enriched Dehalococcoides-containing culture. *Wat Res* **41**: 355–364.

Friis, A.K., Kofoed, J.L., Heron, G., Albrechtsen, H.J., and Bjerg, P.L. (2007c) Microcosm evaluation of bioaugmentation after field-scale thermal treatment of a TCE-contaminated aquifer. *Biodegradation* **18**: 661–674.

Fuchs, G. (2011). Alternative pathways of carbon dioxide fixation: Insights into the early evolution of life?. *Annu Rev Microbiol* **65**: 631–658.

Garcia, F.C., Bestion, E., Warfield, R., and Yvon-Durocher, G. (2018) Changes in temperature alter the relationship between biodiversity and ecosystem functioning. *Proc Natl Acad Sci U S A* **115**: 10989–10994.

Geng, Y., Baumann, F., Song, C., Zhang, M., Shi, Y., Kuhn, P., *et al*. (2017) Increasing temperature reduces the coupling between available nitrogen and phosphorus in soils of Chinese grasslands. *Sci Rep* **7**: 43524.

Gieg, L.M., Davidova, I.A., Duncan, K.E., and Suflita, J.M. (2010). Methanogenesis, sulfate reduction and crude oil biodegradation in hot Alaskan oilfields. *Environ Microbiol* **12**: 3074–3086.

Gong, S., Zhang, T., and Guo, J. (2019) Warming and nitrogen addition change the soil and soil microbial biomass C: N:P stoichiometry of a Meadow Steppe. *Int J Environ Res Public Health* **16**: 2705.

Grigoryan, A.A., Jalique, D.R., Medihala, P., Stroes-Gascoyne, S., Wolfaardt, G.M., McKelvie, J., *et al*. (2018) Bacterial diversity and production of sulfide in microcosms containing uncompacted bentonites. *Heliyon* **4**: e00722.

Head, I.M., Gray, N.D., and Larter, S.R. (2014) Life in the slow lane; biogeochemistry of biodegraded petroleum containing reservoirs and implications for energy recovery and carbon management. *Front Microbiol* **5**: 566.

Heatroadmapeurope (2019). "The Legacy of Heat Roadmap Europe 4 (facts and figures) - Scenarios, recommendations and resources for decarbonising the heating & cooling sector in Europe and complementing the strategic long-term vision of the EU." URL https://heatroadmap.eu/wp-content/uploads/2019/02/HRE_Final-Brochure_web.pdf

Hessler, T., Harrison, S.T.L., and Huddy, R.J. (2020) Linking performance and microbial ecology in a biological sulphate reducing reactor system with biomass retention developed for the treatment of acid rock drainage. *Hydrometallurgy* **197**: 105471.

Heuer, V.B., Krüger, M., Elvert, M., and Hinrichs, K.-U. (2010) Experimental studies on the stable carbon isotope biogeochemistry of acetate in lake sediments. *Org Geochem* **41**: 22–30.

Higashioka, Y., Kojima, H., and Fukui, M. (2011) Temperature-dependent differences in community structure of bacteria involved in degradation of petroleum hydrocarbons under sulfate-reducing conditions. *J Appl Microbiol* **110**: 314–322.

Ho, T.Y., Scranton, M.I., Taylor, G.T., Varela, R., Thunell, R. C., and Muller-Karger, F. (2002) Acetate cycling in the water column of the Cariaco Basin: Seasonal and vertical variability and implication for carbon cycling. *Limnol Oceanogr* **47**: 1119–1128.

Hossain, M.B., Rahman, M.M., Biswas, J.C., Miah, M.M.U., Akhter, S., Maniruzzaman, M., *et al*. (2017) Carbon mineralization and carbon dioxide emission from organic matter added soil under different temperature regimes. *Int J Recycl Org Waste Agricul* **6**: 311–319.

Huang, L., Hwang, A., and Phillips, J. (2011) Effect of temperature on microbial growth rate-mathematical analysis: the Arrhenius and Eyring-Polanyi connections. *J Food Sci* **76**: E553–E560.

Imachi, H., Sakai, S., Lipp, J.S., Miyazaki, M., Saito, Y., Yamanaka, Y., *et al*. (2014) *Pelolinea submarina* gen.

nov., sp. nov., an anaerobic, filamentous bacterium of the phylum Chloroflexi isolated from subseafloor sediment. *Int J Syst Evol Microbiol* **64**: 812–818.

Isaksen, M.F., Bak, F., and Jørgensen, B.B. (1994) Thermophilic sulfate-reducing bacteria in cold marine sediment. *FEMS Microbiol Ecol* **14**: 1–8.

Jesußek, A., Köber, R., Grandel, S., and Dahmke, A. (2012) Aquifer heat storage: sulphate reduction with acetate at increased temperatures. *Environ Earth Sci* **69**: 1763–1771.

Jesußek, A., Grandel, S., and Dahmke, A. (2013) Impacts of subsurface heat storage on aquifer hydrogeochemistry. *Environ Earth Sci* **69**: 1999–2012.

Jiao, F., Shi, X.R., Han, F.P., and Yuan, Z.Y. (2016) Increasing aridity, temperature and soil pH induce soil C-N-P imbalance in grasslands. *Sci Rep* **6**: 19601.

Jones, D.M., Head, I.M., Gray, N.D., Adams, J.J., Rowan, A. K., Aitken, C.M., *et al*. (2008). Crude-oil biodegradation via methanogenesis in subsurface petroleum reservoirs. *Nature* **451**: 176–180.

Jungbluth, S.P., Glavina Del Rio, T., Tringe, S.G., Stepanauskas, R., and Rappe, M.S. (2017) Genomic comparisons of a bacterial lineage that inhabits both marine and terrestrial deep subsurface systems. *Peer J* **5**: e3134.

Kallesøe, A.J., and Vangkilde-Pedersen, T. (eds). 2019: Underground Thermal Energy Storage (UTES) – state-of-the-art, example cases and lessons learned. HEATSTORE project report, GEOTHERMICA – ERA NET Cofund Geothermal. 130 pp + appendices. URL https://www.heatstore.eu/documents/HEATSTORE_UTES%20State%20of%20the%20Art_WP1_D1.1_Final_2019.04.26.pdf

Kallmeyer, J., and Boetius, A. (2004) Effects of temperature and pressure on sulfate reduction and anaerobic oxidation of methane in hydrothermal sediments of Guaymas Basin. *Appl Environ Microbiol* **70**: 1231–1233.

Karnachuk, O.V., Frank, Y.A., Lukina, A.P., Kadnikov, V.V., Beletsky, A.V., Mardanov, A.V., *et al*. (2019) Domestication of previously uncultivated Candidatus Desulforudis audaxviator from a deep aquifer in Siberia sheds light on its physiology and evolution. *ISME J* **13**: 1947–1959.

Klemps, R., Cypionka, H., Widdel, F., and Pfennig, N. (1985) Growth with hydrogen, and further physiological characteristics of *Desulfotomaculum* species. *Arch Microbiol* **143**: 203–208.

Koelschbach, J.S., Mouttaki, H., Pickl, C., Heipieper, H.J., Rachel, R., Lawson, P.A., *et al*. (2017) Rectinema cohabitans gen. nov., sp. nov., a rod-shaped spirochaete isolated from an anaerobic naphthalene-degrading enrichment culture. *Int J Syst Evol Microbiol* **67**: 1288–1295.

Koproch, N., Dahmke, A., and Kober, R. (2019) The aqueous solubility of common organic groundwater contaminants as a function of temperature between 5 and 70 degrees C. *Chemosphere* **217**: 166–175.

Lerm, S., Westphal, A., Miethling-Graff, R., Alawi, M., Seibt, A., Wolfgramm, M., *et al*. (2013) Thermal effects on microbial composition and microbiologically induced corrosion and mineral precipitation affecting operation of a geothermal plant in a deep saline aquifer. *Extremophiles* **17**: 311–327.

Liu, F., and Conrad, R. (2010) Thermoanaerobacteriaceae oxidize acetate in methanogenic rice field soil at 50 degrees C. *Environ Microbiol* **12**: 2341–2354.

Lueders, T. (2017). The ecology of anaerobic degraders of BTEX hydrocarbons in aquifers. *FEMS Microbiol Ecol* **93**: fiw220.

Madigan, M.T., Bender, K.S., Buckley, D.H., Sattley, W.M., and Stahl, D.A. (2017) *Brock: Biology of Microorganisms*. New York, NY: Pearson.

Magot, M., Fardeau, M.L., Arnauld, O., Lanau, C., Ollivier, B., Thomas, P., *et al*. (1997) *Spirochaeta smaragdinae* sp. nov., a new mesophilic strictly anaerobic spirochete from an oil field. *FEMS Microbiol Lett* **155**: 185–191.

Meckenstock, R.U., Elsner, M., Griebler, C., Lueders, T., Stumpp, C., Aamand, J., *et al*. (2015) Biodegradation: Updating the concepts of control for microbial cleanup in contaminated aquifers. *Environ Sci Technol* **49**: 7073–7081.

Metze, D., Popp, D., Schwab, L., Keller, N.-S., da Rocha, U. N., Richnow, H.-H., and Vogt, C. (2021). Temperature management potentially affects carbon mineralization capacity and microbial community composition of a shallow aquifer. *FEMS Microbiol Ecol* **97**: fiaa261.

Miao, Z., Brusseau, M.L., Carroll, K.C., Carreon-Diazconti, C., and Johnson, B. (2012) Sulfate reduction in groundwater: characterization and applications for remediation. *Environ Geochem Health* **34**: 539–550.

Min, H., and Zinder, S.H. (1990) Isolation and characterization of a thermophilic sulfate-reducing bacterium Desulfotomaculum thermoacetoxidans sp. nov. *Arch Microbiol* **153**: 399–404.

Mohr, P.W., and Krawiec, S. (1980) Temperature characteristics and Arrhenius plots for nominal psychrophiles, mesophiles and thermophiles. *Microbiology* **12**: 311–317.

Muller, S., Vogt, C., Laube, M., Harms, H., and Kleinsteuber, S. (2009) Community dynamics within a bacterial consortium during growth on toluene under sulfate-reducing conditions. *FEMS Microbiol Ecol* **70**: 586–596.

National Research Council. (2000) *Natural Attenuation for Groundwater Remediation*. Washington, DC: The National Academies Press.

Ni, Z., van Gaans, P., Smit, M., Rijnaarts, H., and Grotenhuis, T. (2015) Biodegradation of cis-1, 2-dichloroethene in simulated underground thermal energy storage systems. *Environ Sci Technol* **49**: 13519–13527.

O'Sullivan, L.A., Roussel, E.G., Weightman, A.J., Webster, G., Hubert, C.R., Bell, E., *et al*. (2015) Survival of desulfotomaculum spores from estuarine sediments after serial autoclaving and high-temperature exposure. *ISME J* **9**: 922–933.

Ozuolmez, D., Moore, E.K., Hopmans, E.C., Sinninghe Damste, J.S., Stams, A.J.M., and Plugge, C.M. (2020) Butyrate conversion by sulfate-reducing and methanogenic communities from anoxic sediments of Aarhus Bay, Denmark. *Microorganisms* **8**: 606.

Pannekens, M., Kroll, L., Muller, H., Mbow, F.T., and Meckenstock, R.U. (2019) Oil reservoirs, an exceptional habitat for microorganisms. *Nat Biotechnol* **49**: 1–9.

Piceno, Y.M., Reid, F.C., Tom, L.M., Conrad, M.E., Bill, M., Hubbard, C.G., *et al*. (2014) Temperature and injection water source influence microbial community structure in four Alaskan North Slope hydrocarbon reservoirs. *Front Microbiol* **5**: 409.

Purkamo, L., Bomberg, M., Nyyssonen, M., Ahonen, L., Kukkonen, I., and Itavaara, M. (2017) Response of deep subsurface microbial community to different carbon sources and electron acceptors during approximately 2 months incubation in microcosms. *Front Microbiol* **8**: 232.

Qiu, Y.L., Sekiguchi, Y., Imachi, H., Kamagata, Y., Tseng, I. C., Cheng, S.S., *et al*. (2003) *Sporotomaculum syntrophicum* sp. nov., a novel anaerobic, syntrophic benzoate-degrading bacterium isolated from methanogenic sludge treating wastewater from terephthalate manufacturing. *Arch Microbiol* **179**: 242–249.

Quast, C., Pruesse, E., Yilmaz, P., Gerken, J., Schweer, T., Yarza, P., *et al*. (2013) The SILVA ribosomal RNA gene database project: improved data processing and web-based tools. *Nucleic Acids Res* **41**: D590–D596.

Rakoczy, J., Schleinitz, K.M., Muller, N., Richnow, H.H., and Vogt, C. (2011) Effects of hydrogen and acetate on benzene mineralisation under sulphate-reducing conditions. *FEMS Microbiol Ecol* **77**: 238–247.

Ranneklev, S.B., and Baath, E. (2001) Temperature-driven adaptation of the bacterial community in peat measured by using thymidine and leucine incorporation. *Appl Environ Microbiol* **67**: 1116–1122.

Robador, A., Muller, A.L., Sawicka, J.E., Berry, D., Hubert, C. R., Loy, A., *et al*. (2016) Activity and community structures of sulfate-reducing microorganisms in polar, temperate and tropical marine sediments. *ISME J* **10**: 796–809.

Rooney-Varga, J.N., Anderson, R.T., Fraga, J.L., Ringelberg, D., and Lovley, D.R. (1999) Microbial communities associated with anaerobic benzene degradation in a petroleum-contaminated aquifer. *Appl Environ Microbiol* **65**: 3056–3063.

Saad, S., Bhatnagar, S., Tegetmeyer, H.E., Geelhoed, J.S., Strous, M., and Ruff, S.E. (2017) Transient exposure to oxygen or nitrate reveals ecophysiology of fermentative and sulfate-reducing benthic microbial populations. *Environ Microbiol* **19**: 4866–4881.

Saito, T., Hamamoto, S., Ueki, T., Ohkubo, S., Moldrup, P., Kawamoto, K., *et al*. (2016) Temperature change affected groundwater quality in a confined marine aquifer during long-term heating and cooling. *Water Res* **94**: 120–127.

Sanner, B., Kabus, F., Seibt, P., and Bartels, J. (2005). "Underground thermal energy storage for the German Parliament in Berlin, system concept and operational experiences", in Proceedings world geothermal congress (Antalya, Turkey.: International Geothermal Association).

Schirmer, M., Dahmke, A., Dietrich, P., Dietze, M., Gödeke, S., Richnow, H.H., *et al*. (2006) Natural attenuation research at the contaminated megasite Zeitz. *J Hydrol* **328**: 393–407.

Stackebrandt, E., Sproer, C., Rainey, F.A., Burghardt, J., Päuker, O., and Hippe, H. (1997) Phylogenetic analysis of the genus Desulfotomaculum: Evidence for the misclassification of desulfotomaculum guttoideum and description of *Desulfotomaculum orientis* as *Desulfosporosinus orientis* gen. nov., comb. nov. *Int J Sys Evol Microbiol* **47**: 1134–1139.

Starke, R., Keller, A., Jehmlich, N., Vogt, C., Richnow, H.H., Kleinsteuber, S., *et al*. (2016) Pulsed (13)C2-acetate protein-SIP unveils epsilonproteobacteria as dominant acetate utilizers in a sulfate-reducing microbial community mineralizing benzene. *Microb Ecol* **71**: 901–911.

Taubert, M., Vogt, C., Wubet, T., Kleinsteuber, S., Tarkka, M.T., Harms, H., *et al*. (2012) Protein-SIP enables time-resolved analysis of the carbon flux in a sulfate-reducing, benzene-degrading microbial consortium. *ISME J* **6**: 2291–2301.

Thauer, R.K., Zinkhan, D.M., and Spormann, A.M. (1989) Biochemistry of acetate catabolism in anaerobic chemotrophic bacteria. *Annu Rev Microbiol* **43**: 43–67.

Tian, H., Gao, P., Chen, Z., Li, Y., Li, Y., Wang, Y., *et al*. (2017) Compositions and abundances of sulfate-reducing and sulfur-oxidizing microorganisms in water-flooded petroleum reservoirs with different temperatures in China. *Front Microbiol* **8**: 143.

Todorov, O., Alanne, K., Virtanen, M., and Kosonen, R. (2020) A method and analysis of aquifer thermal energy storage (ATES) system for district heating and cooling: A case study in Finland. *Sust Cit Soc* **53**: 101977:1 –101977:15.

USEPA (1999). "Use of monitored natural attenuation at superfund, RCRA corrective action and underground storage tank sites. OSWER Directive Number 9200.4-17P", (ed.) O.o.S.W.a.E. Response. Washington (DC).

Velji, M.I., and Albright, L.J. (1984). "The dispersion of adhered marine bacteria by pyrophosphate and ultrasound prior to direct counting", in: 2. Colloque International de Bacteriologie Marine, Brest (France).

Vogt, C., Godeke, S., Treutler, H.C., Weiss, H., Schirmer, M., and Richnow, H.H. (2007) Benzene oxidation under sulfate-reducing conditions in columns simulating in situ conditions. *Biodegradation* **18**: 625–636.

Widdel, F., and Bak, F. (2006) The Genus Bacillus—Nonmedical. In *The Prokaryotes*, 3rd ed, Dworkin, M., Falkow, S., Rosenberg, E., Schleifer, K., and Stackebrandt, E. (eds). New York, NY: Springer, pp. 787–794.

Widdel, F., and Pfennig, N. (1977) A new anaerobic, sporing, acetate-oxidizing, sulfate-reducing bacterium, Desulfotomaculum (emend.) acetoxidans. *Arch Microbiol* **112**: 119–122.

Wu, H., Green, M., and Scranton, M.I. (1997) Acetate cycling in the water column and surface sediment of Long Island Sound following a bloom. *Limnol Oceanogr* **42**: 705–713.

Yadav, B.K., Shrestha, S.R., and Hassanizadeh, S.M. (2012) Biodegradation of toluene under seasonal and diurnal fluctuations of soil-water temperature. *Water Air Soil Pollut* **223**: 3579–3588.

Yi, Y., Wang, H., Chen, Y., Gou, M., Xia, Z., Hu, B., *et al*. (2020) Identification of novel butyrate- and acetate-oxidizing bacteria in butyrate-fed mesophilic anaerobic chemostats by DNA-based stable isotope probing. *Microb Ecol* **79**: 285–298.

Yilmaz, P., Parfrey, L.W., Yarza, P., Gerken, J., Pruesse, E., Quast, C., *et al*. (2014) The SILVA and "All-species Living Tree Project (LTP)" taxonomic frameworks. *Nucleic Acids Res* **42**: D643–D648.

Zeman, N.R., Irianni Renno, M., Olson, M.R., Wilson, L.P., Sale, T.C., and De Long, S.K. (2014) Temperature

impacts on anaerobic biotransformation of LNAPL and concurrent shifts in microbial community structure. *Biodegradation* **25**: 569–585.

Zouch, H., Karray, F., Armougom, F., Chifflet, S., Hirschler-Rea, A., Kharrat, H., *et al*. (2017) Microbial diversity in sulfate-reducing marine sediment enrichment cultures associated with anaerobic biotransformation of coastal stockpiled phosphogypsum (Sfax, Tunisia). *Front Microbiol* **8**: 1583.

Supporting Information

Additional Supporting Information may be found in the online version of this article at the publisher's web-site:

Fig. S1. Two bottles, Zz-O1 and Zz-O2 used to further setup the six enrichment cultures Zox1-6. Most of the upper layers were discarded before consolidation of the darker layers.

Fig. S2. Rarefaction analysis of the 18 replicates sequenced.

Fig. S3. Microbial community compositions of treatments: 5 (45° → 12 → 45°C), 6 (45 → 25 → 45°C), 7 (45 → 38 → °C) and 8 (45 → 60 → 45°C), represented at the order level, with the corresponding class level in parentheses. 'Replicate' and 'Label' information correspond to the replicate described in Table S2.

Fig. S4. Microbial community of the replicates sacrificed at various stages of the heat exchange, that is pre-heat exchange ($d = 6$), post ($d = 35$) and at the end of the experiment ($d = 120$ and $d = 82$). Sequences are represented at the order level, with the class level represented in parenthesis.

Fig. S5. Summary of the workflow for enrichment of a community able to mineralize acetate at 45°C (culture bottle Zox4, used as the inoculum in this study), and the setup of differently treated replicate cultures in subsequent heat exchange experiments. Sterile controls are indicated by skulls. There are no replicates for labels 4.08, 4.12, and 4.16 as no sterile replicates were set up for treatment 2, treatment 3, and treatment 4 respectively.

Fig. S6. Shannon diversity index for twelve replicates including 4.03 to 4.31 in descending order.

Fig. S7. Diversity indices for replicates including 4.38 to 4.36 (A) and 4.35 to 4.33 (B) in descending order according to the stage of sacrifice. Replicate 4.03 was included as reference.

Fig. S8. PCoA of the 18 replicates from treatments 1-8, S1, and S2. Points are represented according to replicate (colour) and cluster (shape). Cluster 1 represents replicates from treatment 1; Cluster 2: 4.07, 4.09, 4.11; Cluster 3: 4.17–4.31; Cluster 4: 4.33–4.35; Cluster 5: 4.36–4.38.

Table S1. Recipe of the modified mineral salt media used for this study.

Table S2. Additional information for individual replicates for each treatment. Experiment in treatment 7 was completed during incubation at 38°C.

Table S3. Additional information for acetate mineralization, sulfide production for each replicate in treatments 1–8.

Table S4. Next relatives of the genera *Spirochaetaceae* member, *Desulfotomaculum* and *Candidatus Desulforudis* member phylotypes in this study for the select replicates, based on BLAST identities of 16S rRNA gene sequences. Phylotypes are arranged based on percent BLAST identity in descending order.